DAMAGE TOLERANCE TECHNOLOGY FOR CURRENT AND FUTURE AIRCRAFT STRUCTURE

Hans-Jürgen Schmidt

Retired from Airbus, now AeroStruc – Aeronautical Engineering

Key words: Damage tolerance, fatigue life, regulations, advanced metallic materials, welding technologies, structural health monitoring.

Abstract. Fatigue and damage tolerance analysis and testing became one of the key means during development, design and maintenance of aircraft structure. This is the result of the increased requirements regarding structural reliability, low weight, low manufacturing costs and low operating costs. Furthermore, any new structure has to fulfill the more stringent actual airworthiness requirements, which will be advanced again to further improve the reliability of the aircraft by providing the so-called large damage capability. This behavior is an additional mean to detect critical structural damages, which were not found during normal maintenance. This lecture gives a brief overview about fatigue and damage tolerance analysis methods for conventional fuselage structure for local and multiple damages as well as examples of major development and certification tests, e.g. curved panel tests, barrel tests and full scale fatigue tests. The increased requirements and expectations led to significant efforts in developing more efficient structures by using advanced monolithic and hybrid materials, new assembly methods and, in the future, by possible application of structural health monitoring. The lecture describes advanced materials, fiber metal laminates, laser beam welding, friction stir welding, bonding / metal laminates and structural health monitoring. The major advantages and disadvantages of these technologies regarding fatigue and damage tolerance are discussed including examples of application. Important fatigue and damage tolerance test results are presented as well as the improved analysis methods, which take into account the new characteristics of the advanced materials and technologies.

1 INTRODUCTION

The primary objective of the aerospace industry is to offer products that not only meet the operating criteria in terms of payloads and range but also significantly reduce the direct operating costs of their customers, the airlines. The structure of the present civil transport aircraft is designed considering the current and forthcoming airworthiness regulations, the customers' requirements and manufacturing aspects.

During the design of aircraft structures a wide range of aspects have to be considered to reach sufficient static strength and excellent fatigue and damage tolerance (F&DT) behavior. The major aspects of the current fatigue and damage tolerance regulation FAR 25.571 Amendment 96 [1] and the corresponding Advisory Circular AC 25.571-1C [2] are:

- "An evaluation of the strength, detail design, and fabrication must show that catastrophic failure due to fatigue, corrosion, manufacturing defects, or accidental damage, will be avoided throughout the operational life of the airplane."
- "Based on the evaluations required by this section, inspections or other procedures must be established, as necessary, to prevent catastrophic failure, ..."

- "It must be demonstrated with sufficient full-scale fatigue test evidence that widespread fatigue damage will not occur within the design service goal of the airplane."

However, the design of a modern transport aircraft should not only consider the regulations applicable at the design phase, but should take into account the forthcoming regulations, which are under discussion or issued as a Notice of Proposed Rule Making (NPRM). The damage tolerance paragraph of FAR 25 has been widely discussed in the General Structures Harmonization Working Group (GSHWG) between the airworthiness authorities and the manufacturers under the umbrella of the Aviation Rulemaking Advisory Committee (ARAC). The major requirements in the future regulation 25.571 [3] and the AC [4] will be:

- "... inspections or other procedures must be established, ... The limit of validity (LOV) of this maintenance program must also be included in the Airworthiness Limitations Section ..."
- "Structural damage capability. ... it must be shown ... that the structure is able to withstand the loads specified... in the presence of damage equivalent to:
  i) the complete failure of any single element, or
  ii) partial failure between damage containment features that significantly retard or arrest a crack ..."
- "For single load path structure, ... SDC requirement shall be achieved through the demonstration of slow crack growth, an upper bound inspection threshold of 50% DSG ..."

Figure 1 shows in principle the damage types to be considered during the damage tolerance evaluation. The basic assumption for all damage tolerance assessments is the local damage scenario, i.e. a damage in one or more elements of a principal structural element (PSE) at a single site, which is not influenced by damages in adjacent locations.

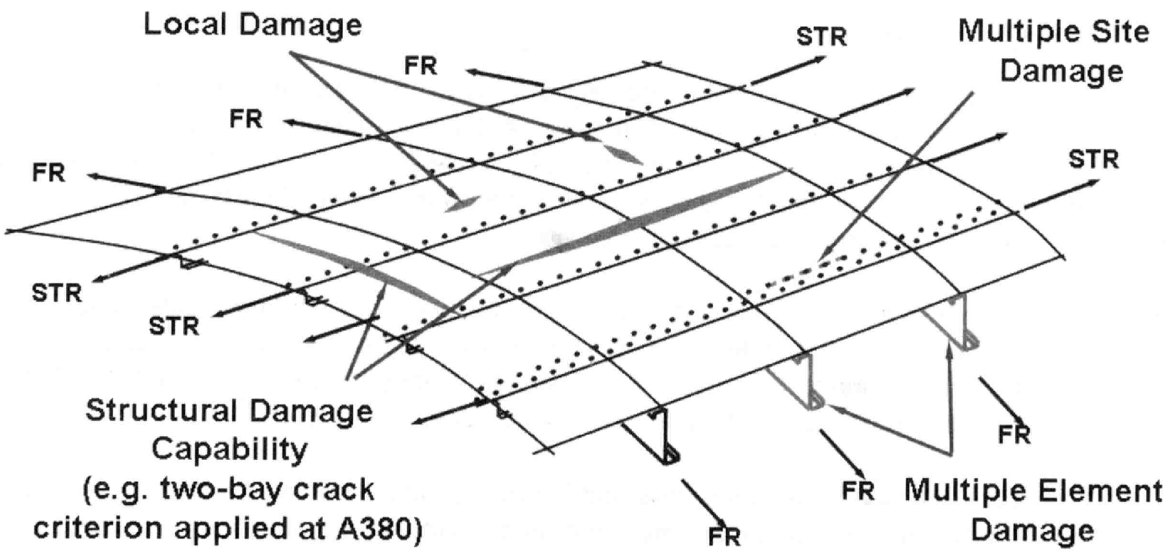

Figure 1: Damage types to be considered during F&DT evaluation – fuselage examples

Furthermore multiple site damage (MSD) and/or multiple element damage (MED) have to be considered in structure susceptible to these types of damages. Details about MSD, MED and resulting widespread fatigue damage (WFD) will be explained later in this paper. The structural damage capability (SDC) will be required by the forthcoming regulations. It is the characteristic of the structure which permits it to retain sufficient static load capability in the presence of damage equivalent to the complete failure of a load path or partial failure of the load path between damage containment features, i.e. a one-bay-crack-criterion. A more detailed interpretation of the regulations and requirements is given by Swift [5]. The fatigue and damage tolerance evaluation has to cover the complete primary structure, which contributes significantly to carrying flight, ground and pressurization loads and those parts of secondary structure, which may affect the primary structure when damaged or failed.

2 FATIGUE AND DAMAGE TOLERANCE ANALYSIS

2.1 General Procedure

Figure 2 gives an overview about the general procedure for the fatigue and damage tolerance analysis. The final goal of the F&DT analysis of damage tolerant structure is the definition of a structural inspection program. The following information has to be provided to ensure an appropriate inspection program, which is effective to guarantee the airworthiness of the structure throughout the operational life:

- Description of inspection area
- Inspection method to be applied
- Inspection threshold (first inspection)
- Repetitive inspection interval

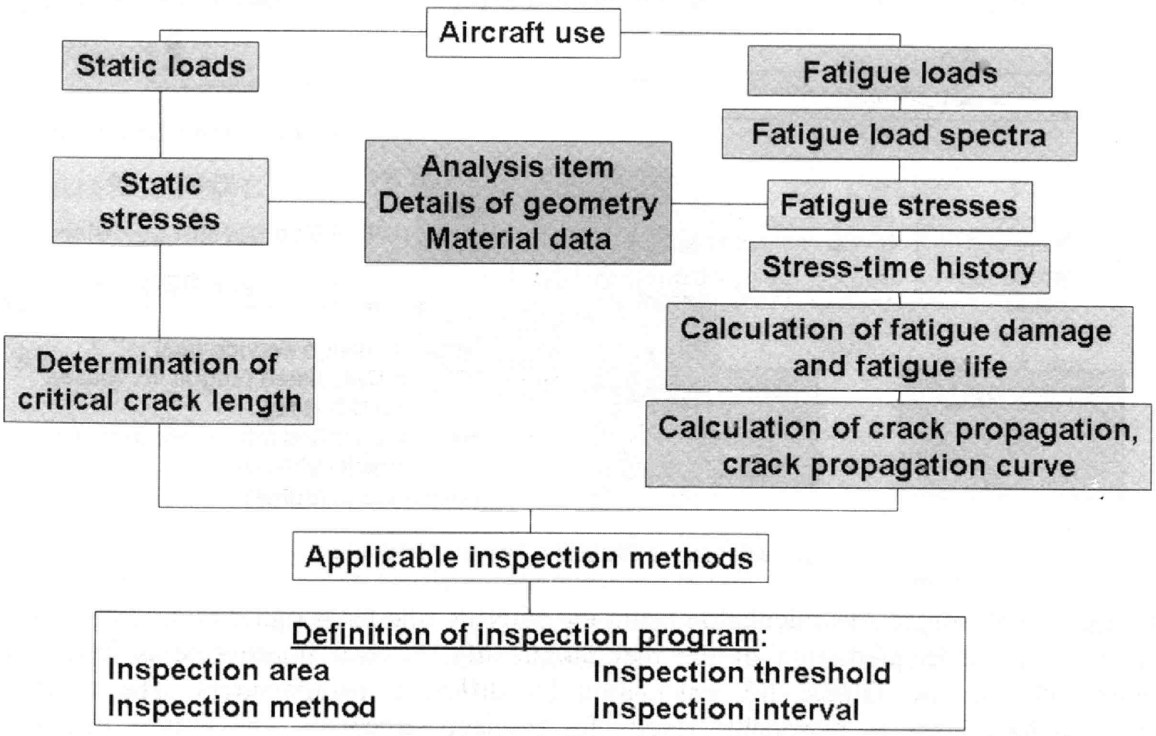

Figure 2: F&DT analysis – general procedure

2.2 Fatigue life analysis for local damages

For safe life structure the fatigue life analysis is an essential part of the certification procedure. Although not required by the regulations for damage tolerant structures fatigue life analyses are performed by all major airframe manufacturers due to the following reasons:

- demonstration of the reliability of the structure up to the design service goal or the extended service goal.
- determination of the inspection threshold instead of using the initial flaw concept for a certain type of "multiple load path and crack arrest 'fail safe' structure".

Figure 3 describes the principles of the fatigue life analysis together with the minimum scatter factors to be applied. The fatigue life analysis determines the period in time up to a detectable fatigue flaw, which is initiated and propagated due to cyclic loading. The major input data, geometry, stress spectrum or stress-time history and the relevant material data (SN diagram, "Wöhler" curve) are the basis for the calculation of the fatigue damage D, which is generally determined for one design service goal (DSG). The resulting fatigue life N = DSG / D is the average value, on which the scatter factor has to be applied. Depending on the type of structure, damage tolerant or safe life, the minimum values are defined and agreed by the airworthiness authorities.

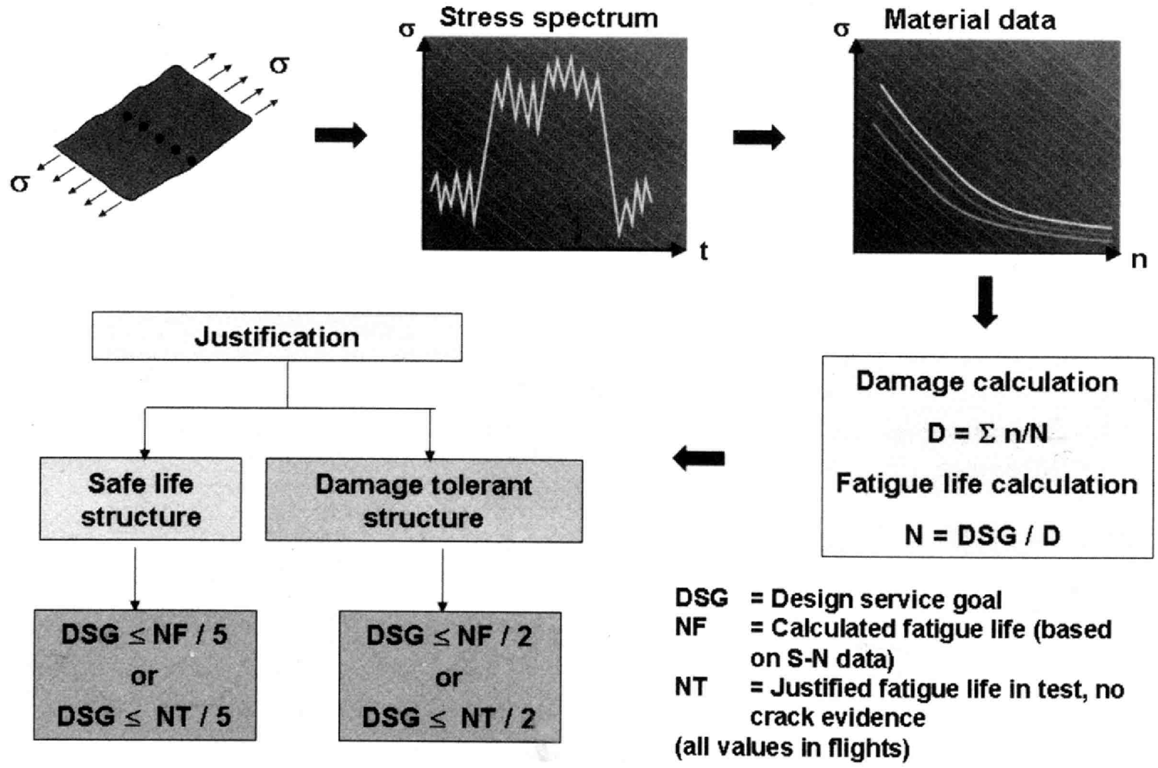

Figure 3: Fatigue life analysis for local damage

The traditional fatigue life calculation using the MINER rule leads either to un-conservative results or an under-prediction of the real fatigue life. Several improvements have been implemented in the fatigue life calculation by different manufacturers. The approach described here leads to reasonable results for fuselage structures. The fatigue life N_E is determined for a required probability of failure:

$$N_E = \frac{DSG \cdot D_F \cdot x}{D_{total} \cdot j_L \cdot R_{50\%}}$$

with:

DSG = Design service goal, fatigue damage is generally determined for one DSG

D_F = Miner factor, to consider failure under variable amplitude loading before fatigue damage is 1.0

x	=	reduction factor, to consider several fatigue critical locations
D_{total}	=	$\Sigma(n/N)$ = total fatigue damage, determined for one DSG (n = applied cycles, N = cycles up to failure from SN data incl. extrapolation)
j_L	=	scatter factor, to consider scatter in load spectra and material data, depending on the required probability of failure
$R_{50\%}$	=	risk factor, to consider limited number of specimens to obtain material (SN) data

2.3 Damage tolerance analysis

The damage tolerance analysis is performed to determine the structural inspection program. It comprises the residual strength analysis and the crack growth analysis. The purpose of the residual strength analysis is to determine the maximum allowable crack length a_c (last point of stability), which corresponds to the static limit load $\sigma_{c,L}$ as required by FAR 25.571. This allowable crack length is also called maximum tolerable crack length or critical crack length. For fuselage structure the conventional procedure based on stress intensity factor solutions and fracture toughness data is generally sufficient, see Figure 4.

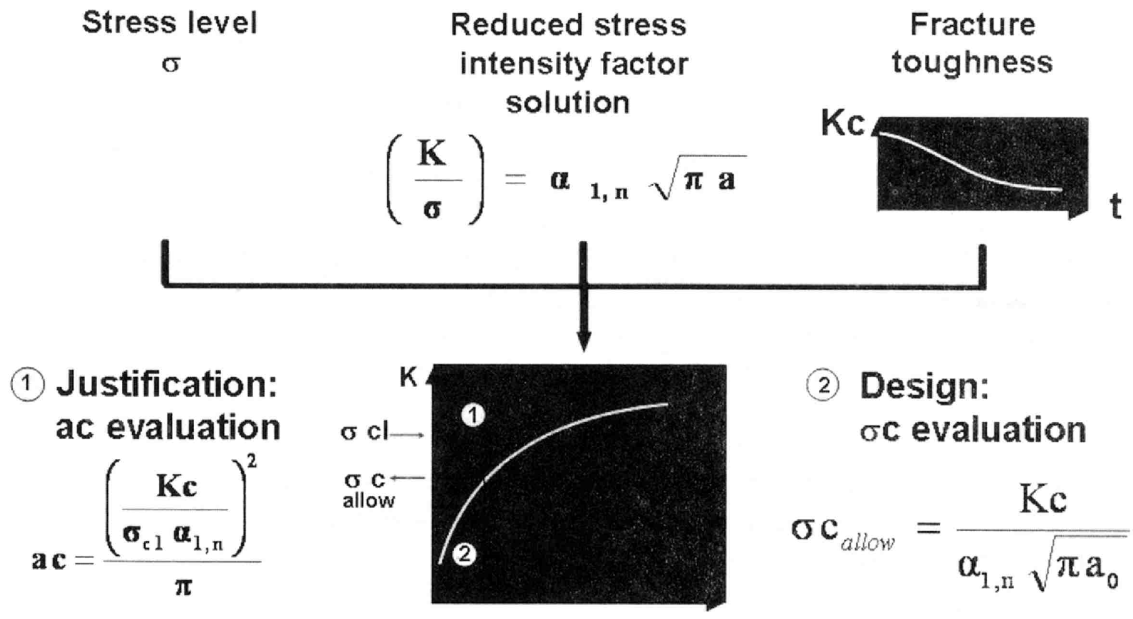

Figure 4: Residual strength analysis

The goal of the crack growth analysis is to determine the crack growth curve between detectable damage size and the critical crack length. Again a conventional linear analysis procedure is generally applied to the fuselage structure as shown in Figure 5. Most often the Forman equation is used for the fuselage structure. In exceptional cases Paris or Walker equation may be chosen.

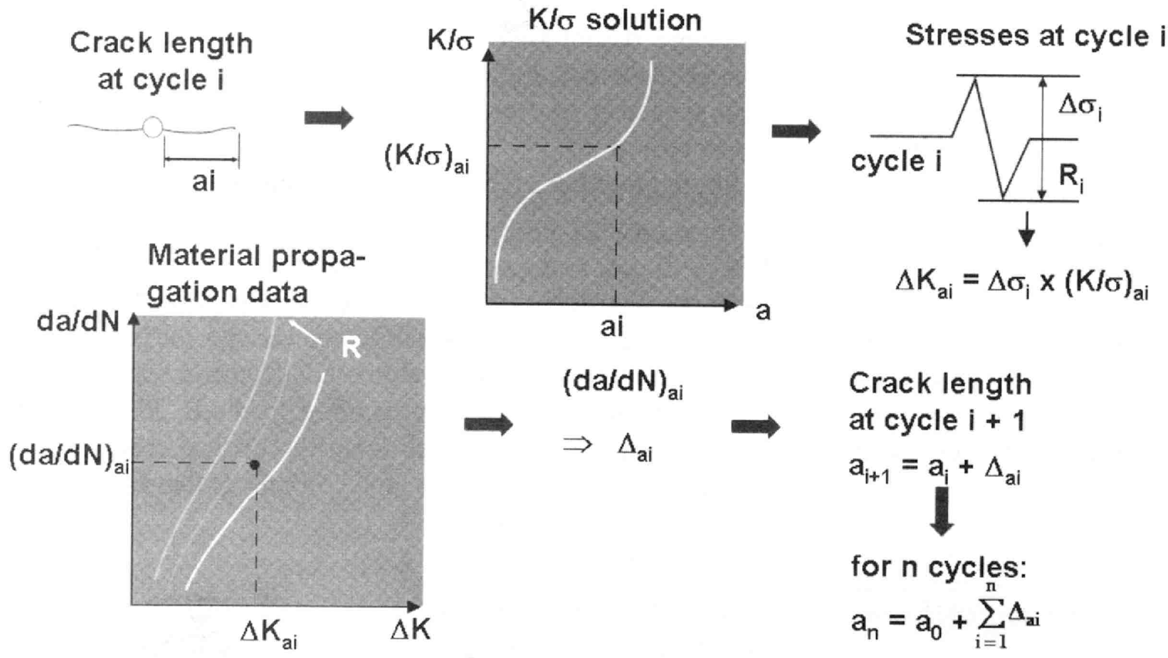

Figure 5: Crack growth analysis

2.4 Damage tolerance analysis of stiffened fuselage panels

For a wide range of simple structures and geometries stress intensity factor solutions are available in the literature, e.g. developed by Rooke Cartwright, Newman Raju, etc. Specific airframe structures such as stiffened panels need more detailed solutions. Fuselage panels, which are stiffened by stringers in aircraft longitudinal direction and frames in circumferential direction, may contain a skin crack and may fail due to either of the following criteria:

- Failure of the skin due to instability of the crack
- Failure of the stiffener perpendicular to the crack due to static strength
- Failure of the fasteners attaching the stiffeners perpendicular to the crack due to exceeding allowable rivet load

Based on the approach from Poe [6,7] and Swift [8,9] a computer code was developed allowing for crack growth and residual strength analysis of a stiffened panel under uni-axial external loading (no bulging). Comparisons of analyses using this code and recent test results from curved stiffened fuselage panels tested under internal pressure and external loads revealed, that the analyses are very conservative for the failure mode crack above broken stiffener. The reason for these differences is the bi-axial loading of the test panels, which is not represented in the analyses. The following features also not considered:

- Flexibility of skin-to-frame joint due to fastener flexibility (and clip connection)
- Bulging of crack fronts due to internal pressure
- Load (stress) distribution between skin and stringers due to internal pressure
- Non-constant stress distribution between frames

Detailed investigation performed by Ahmed and van den Nieuwendijk [10] led to the conclusion that the method mentioned above should be modified to account for effects not considered to date.

2.4.1 Flexibility of skin-to-frame joint

The flexibility of the skin-to-frame connection using a shear clip is based on the total deflection of this joint, see Figure 6.

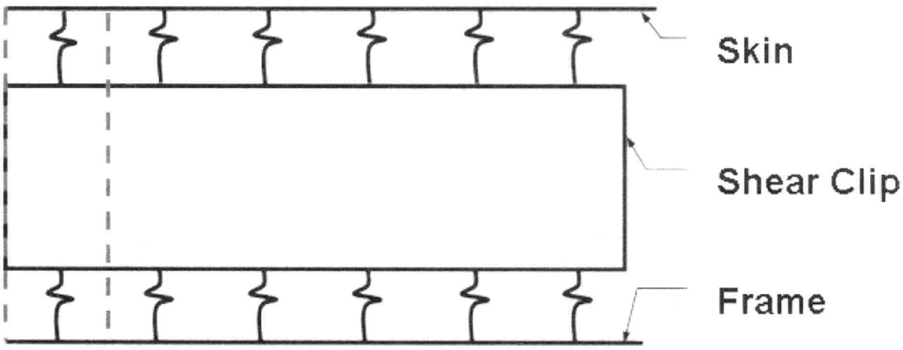

Figure 6: Skin-to-frame joint with clip connection

The total deflection of this joint is the summation of the single deflections:

$$\delta_{\text{total}} = \delta_{\text{rivet skin-clip}} + \delta_{\text{rivet frame-clip}} + \delta_{\text{shear clip}}$$

The flexibilities depend on the applied load, the geometries of skin, frame, clip and fasteners as well as on the material data for fasteners, skin, frame and clip.

2.4.2 Bulging of crack fronts

Bulging of the crack fronts is a phenomenon, which occurs at longitudinal cracks in pressure vessels. It is the displacement of the crack fronts outside of the contour of the structure, see Figure 7.

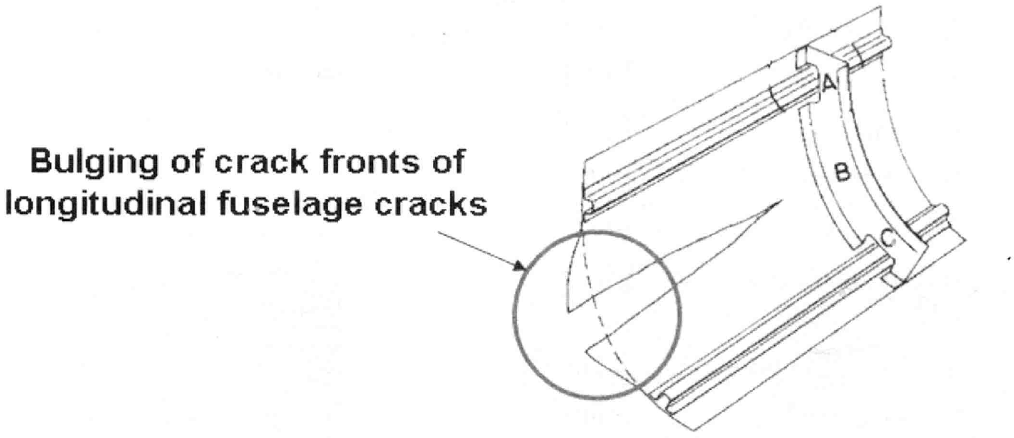

Figure 7: Phenomenon of bulging

The correction for the stress intensity factor solution is described by:

For longitudinal crack above broken frame:

$$\beta_{\text{BULGING}} = 1 + \frac{10\,a}{R} \cos\left(\frac{\pi\,a}{2\,L}\right) \qquad 0 \leq 2a \leq 2L$$

For longitudinal crack between intact frames:

$$\beta_{BULGING} = 1 + \frac{10\,a}{R} \; \frac{\left[1 + \cos\left(\frac{2\pi\, a}{L}\right)\right]}{2} \qquad 0 \le a \le L$$

with:

L	=	distance between stiffeners
R	=	shell radius
a	=	distance from frame to crack tip (for crack above broken frame)
	=	distance from center of bay to crack tip (for crack between intact frames)

2.4.3 Load distribution between skin and stringers

In the current code it is assumed, that the longitudinal skin stress in the middle of the bay is equal to the stringer stress. Flugge's equations [11] show a significant difference in the stringer stress and longitudinal skin stress. These equations for the load flow and the stress, which account for circumferential and axial (longitudinal) stiffening material, are listed below:

$$N_\varphi = P \cdot R \quad [\text{N/mm}]$$
$$N_X = P \cdot R/2 \quad [\text{N/mm}]$$

Skin axial (longitudinal) stress:

$$\sigma_S = \frac{t_\varphi\, N_x + \upsilon\,(t_X - t)\, N_\varphi}{(1-\upsilon^2)\, t_\varphi\, t_X + \upsilon^2\, t\,(t_\varphi + t_X - t)} \qquad [\text{N/mm}^2]$$

with:

t_X	$t_X = t + A_L/S$	[mm]
t_φ	$t_\varphi = t + A_F/L$	[mm]
t	Skin thickness	[mm]
A_L	Longeron area	[mm²]
A_F	Frame area	[mm²]
S	Longeron spacing	[mm]
L	Frame spacing	[mm]
P	Internal cabin pressure	[N/mm²]
R	Shell radius	[mm]
υ	Poisson's ratio	

Stringer (longeron) stress:

$$\sigma_L = \frac{\left[(1-\upsilon^2)\, t_\varphi + \upsilon^2\, t\right] N_x - \upsilon\, t\, N_\varphi}{(1-\upsilon^2)\, t_\varphi\, t_X + \upsilon^2\, t\,(t_\varphi + t_X - t)} \qquad [\text{N/mm}^2]$$

2.4.4 Correction of stiffener area

The effects of joint flexibility and load (stress) distribution between skin and stringers are considered in the method mentioned above by modifying the stiffener areas, i.e. the area of the frame and the area of the stringer, respectively, which are input data to the computer code. For the analysis of longitudinal cracks the frame area is modified such that the frame axial flexibility is compatible with flexibility of the skin to frame joint:

$$A_{\text{frame effective}} = \frac{L_{FS}}{E_{\text{frame}} \cdot \delta_{TOTAL}}$$

with:

L_{FS} = frame segment per rivet pitch
E = Young's modulus
δ_{TOTAL} = total displacement of skin to frame joint per unit force

For circumferential cracks the stringer area is modified considering the stress levels in skin and stringer:

$$A_{\text{stringer effective}} = A_{\text{stringer}} \cdot \frac{\sigma_{\text{skin external}}}{\sigma_{\text{skin total}}} + A_{\text{stringer}} \cdot \frac{\sigma_{\text{stringer }\Delta p}}{\sigma_{\text{skin total}}}$$

with:

A_{stringer} = true stringer area
$\sigma_{\text{skin external}}$ = skin stress due to external loads
$\sigma_{\text{skin total}}$ = total skin stress
$\sigma_{\text{stringer }\Delta p}$ = stringer stress due to internal pressure (acc. to Flugge's equation)

2.4.5 Verification by component tests

The method modified by introduction of the effects described above was verified by comparisons of analysis and test results. The analysis results for longitudinal cracks were verified by curved panel tests loaded by internal pressure and the results for circumferential cracks were compared with test results from flat panels, see Figure 8.

Curved panels loaded by internal pressure as well as external longitudinal and circumferential loads

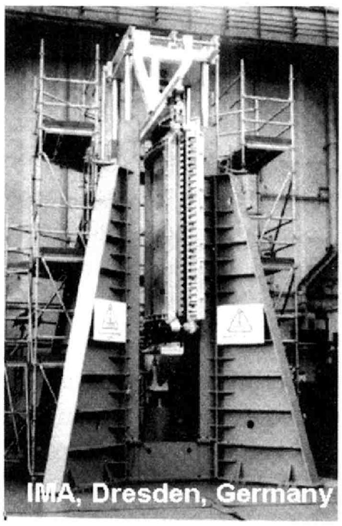

Flat panels with seven stringers to simulate behavior of circumferential cracks

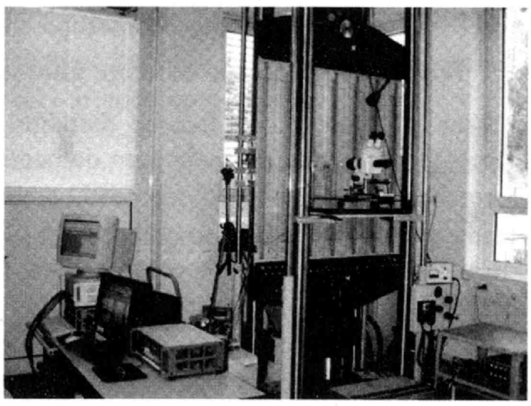

Figure 8: Verification tests for stiffened panel analysis

The results of the comparison are presented in Figure 9 for a longitudinal crack above a broken frame and in Figure 10 for a circumferential crack above a broken stringer.

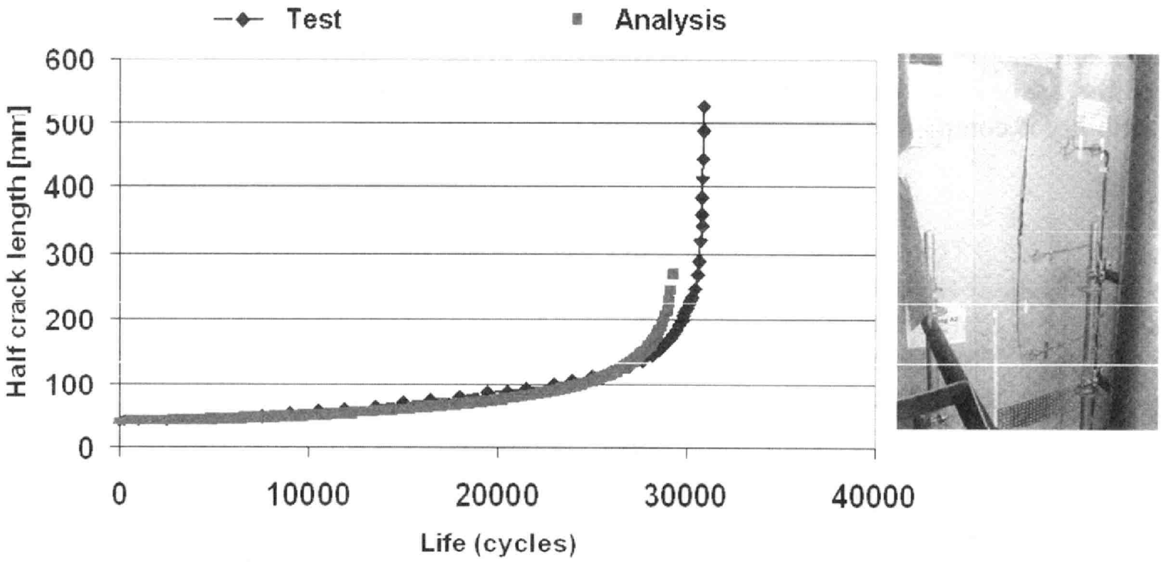

Figure 9: Curved panel test - longitudinal crack above broken frame

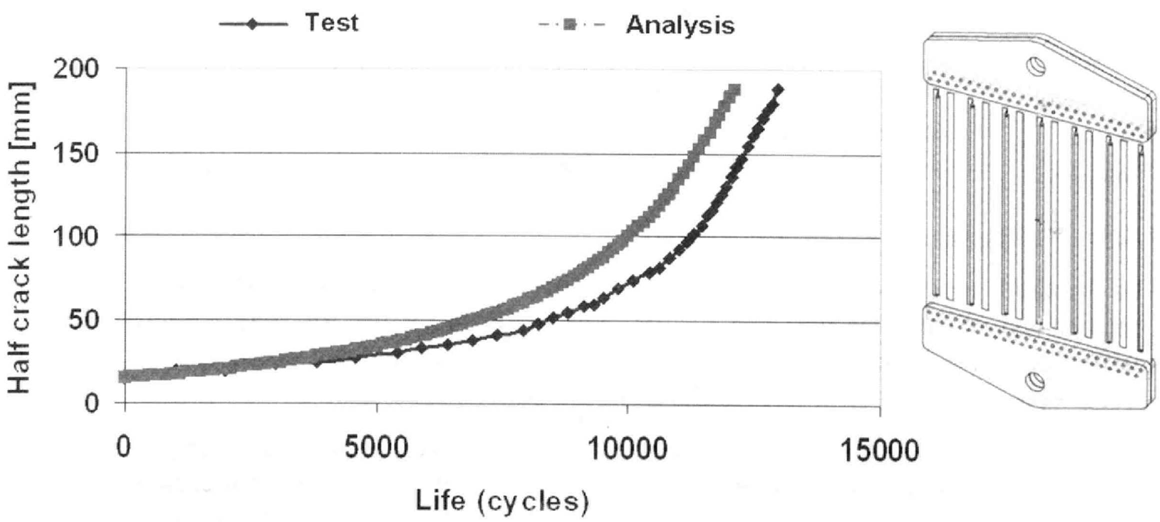

Figure 10: Flat panel test - circumferential crack above broken stringer

2.5 Widespread fatigue damage analysis

The issue of widespread fatigue damage (WFD), which may develop from multiple site damage (MSD) or multiple element damage (MED) is one of the major concerns for an aging airplane fleet, because MSD and MED have a significant influence of the structural behavior. Since the introduction of Amendment 96 of FAR 25 a widespread fatigue damage evaluation has to be performed for new certifications too. WFD, MSD and MED are defined according AC 25.571-1C as:

- Multiple Site Damage, MSD, is a source of widespread fatigue damage characterized by the simultaneous presence of fatigue cracks in the same structural element (i.e. fatigue cracks that may coalesce with or without other damage leading to a loss of required residual strength).

- Multiple Element Damage, MED, is a source of widespread fatigue damage characterized by the simultaneous presence of fatigue cracks in similar adjacent structural elements.
- Widespread Fatigue Damage, WFD, in a structure is characterized by the simultaneous presence of cracks at multiple structural details that are of sufficient size and density whereby the structure will no longer meet its damage tolerance requirement (i.e., to maintain its required residual strength after partial structural failure).

MSD and MED are illustrated in Figure 11.

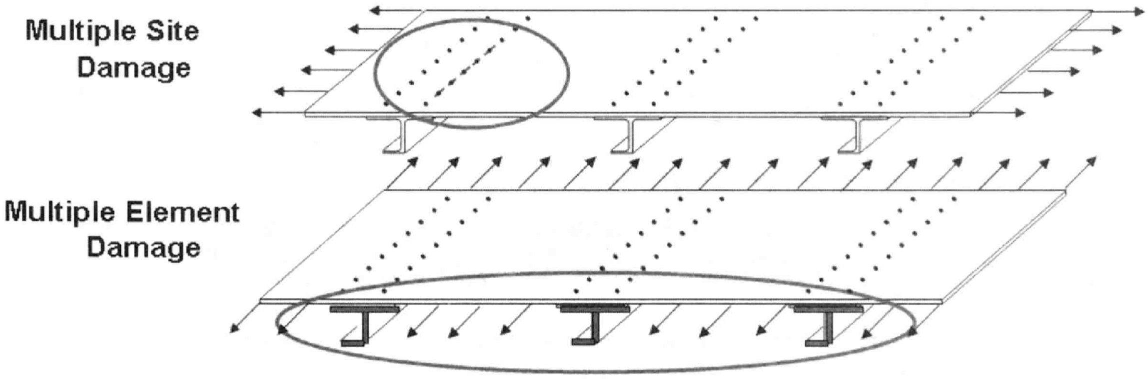

Figure 11: Multiple site damage (MSD) and multiple element damage (MED)

2.5.1 WFD parameters and monitoring period

For aging airplane fleets it is allowed to maintain the airworthiness of the structure by inspections during a certain time period, the so-called Monitoring Period. The monitoring period is defined according to [12] as "the period of time when special inspections of the fleet are initiated due to an increased risk of MSD/MED, and ending when the Structural Modification Point (SMP) is established". This concept could be used in all situations where MSD/MED crack growth is detectable before the structure loses its required residual strength. Figure 12 depicts how a Monitoring Period might be established for an area of structure that meets the criterion of detectable MSD/MED. There are several points that are essential in establishing this period. First is the establishing of the SMP, which is a point reduced from the expected average behavior. Beyond this point the airplane may not be operated without repair, modification or replacement. This point provides equivalent protection as a two-life-time fatigue test. Repeat inspection intervals are established based on the time from detectable fatigue cracks to the average WFD (average behavior) divided by a factor.

For aircraft to be certified according to the current regulation FAR 25.571 Amendment 96 it has to be demonstrated, that WFD will not occur within the design service goal (DSG) of the aircraft. This means, that the SMP has to be greater than the DSG. Special inspections to detect MSD or MED may be performed starting at the ISP.

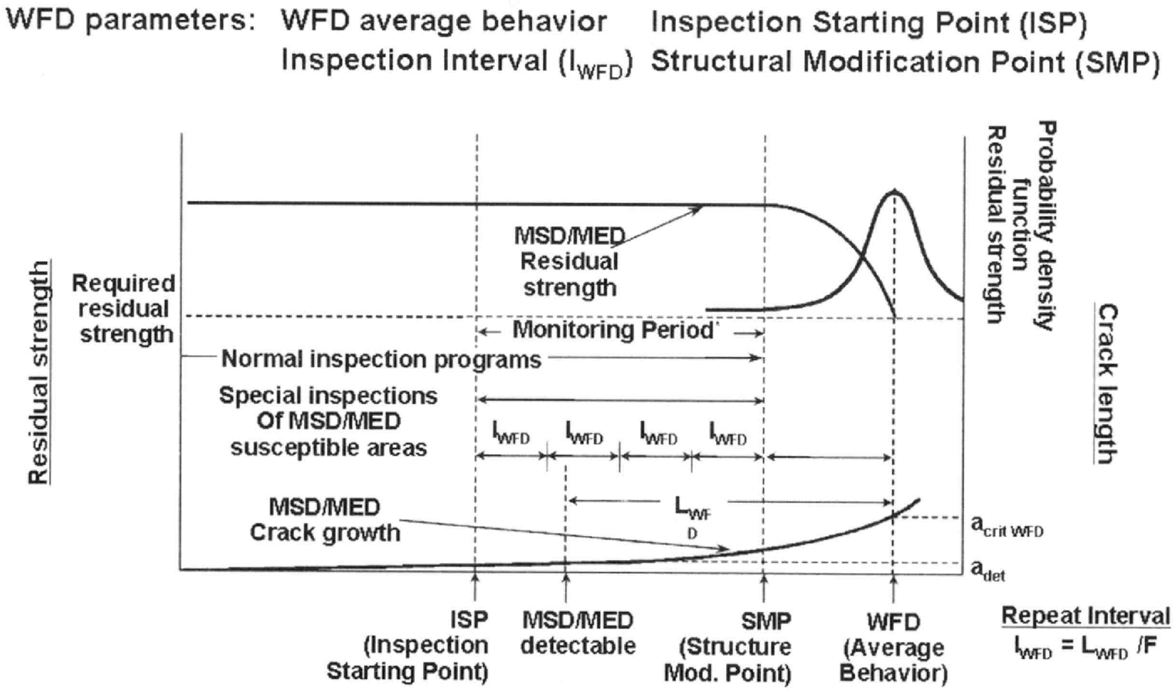

Figure 12: Determination of WFD parameters and monitoring period

2.5.2 Analysis method for WFD

In frame of the European research program Brite-EuRam a project 'Structural maintenance of Ageing Aircraft' (SMAAC) was partly founded by the European Commission during which analysis tools for WFD evaluation were developed. Some additional effort was spent to derive engineering tools for the Airbus fuselage structure to be evaluated, see Figure 13. The development of these engineering tools was supported by extensive testing.

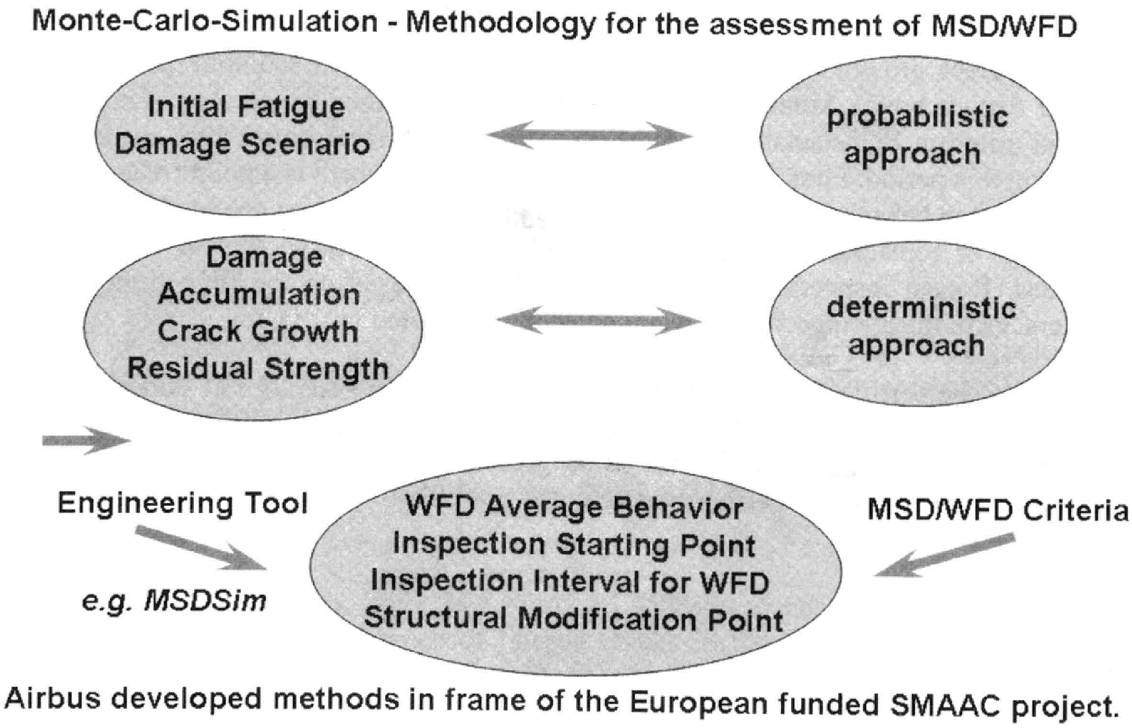

Figure 13: WFD analysis method

There is general agreement throughout the literature that MSD and its subsequent phenomenon WFD largely depend on probabilistic effects. These effects can be derived from parameters which influence the development of MSD and WFD and which themselves show a probabilistic character. The major parameters are the initial design of a structural part, the loading (e.g. high tension, high induced bending or high load transfer), the manufacturing process, the material properties and to a certain degree the environment. These parameters obviously have a great influence on the fatigue life (MSD behavior) of a structure. Therefore, any approach to assess MSD has to consider the probabilistic nature of these parameters.

In the approach developed [13,14,15] this is done by means of a Monte-Carlo simulation. The analysis model itself consists of two parts, a probabilistic and a deterministic part. Within the probabilistic algorithm the initial damage scenario is determined, while the subsequent steps, such as damage accumulation, crack growth and residual strength are calculated in a deterministic approach. The process is performed for a pre-defined number of simulations.

For the probabilistic part of the model, i.e. the calculation of the initial damage scenario, some assumptions have to be made. The model assumes that for a specific structural part the mean fatigue life for a single rivet pitch or a single rivet hole and the scatter of fatigue life in terms of standard deviation are known from fatigue tests with relevant coupons. To assess multiple-hole structures it is assumed that these data can be extrapolated in order to derive a damage scenario for a complete structural item containing many holes. It is also assumed that the fatigue life is distributed according to a log normal distribution, which provides the condition to use an ordinary, fast random generator to determine the initial damage scenario. The principle of generating the initial damage scenario is shown in Figure 14.

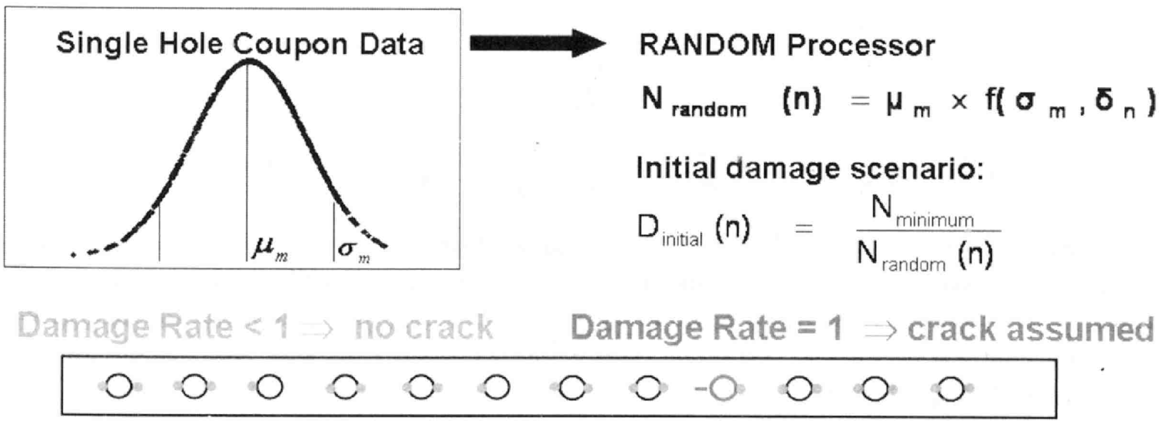

Figure 14: WFD analysis – initial damage scenario

The random processor provides a smooth distribution of random numbers [δ] in the interval [0,1]. Then the fatigue life per site $N_{random}(n)$ is a function of the mean value μ_m, the standard deviation σ_m and the random number δ_n:

$$N_{random}(n) = \mu_m \times f(\sigma_m, \delta_n)$$

The first crack initiation occurs at the location with the lowest $N_{random(n)}$ (=$N_{minimum}$). At this location the damage rate is 1 at time of crack initiation; a 1 mm crack is assumed. According to the fatigue lives obtained from the random generator each crack initiation site n is set to an initial damage percentage $D_{initial}$ [0-100%] depending on the ratio between the minimum of all generated fatigue lives $N_{minimum}$ and the fatigue life of the special site $N_{random}(n)$,

$$D_{initial}(n) = \frac{N_{minimum}}{N_{random}(n)}$$

While the initiated crack starts growing, the other possible initiation sites still have to accumulate more fatigue damage. The damage accumulation is calculated by the equation given below, where $D_{initial}$ is the initial damage, N is the actual number of crack growth cycles and N'_{random} is the fatigue life of damage location n:

$$\text{Damage}(n) = D_{initial}(n) + \frac{N}{N'_{random}(n)}$$

With a time stepping routine, which simulates the fatigue cycling, the damage rate of each location is checked and new cracks are initiated where the accumulated damage reaches 100 percent. In the same time stepping routine the crack propagation of the initiated cracks is calculated. In each step the net stress is recalculated to account for the stress increase due to crack extension. The stress increase consequently affects the damage accumulation procedure, since higher stress values lead to lower fatigue life of the single initiation sites, i.e. than term N_{random} decreases leading to N'_{random}. Furthermore, N'_{random} includes effects from a crack at the other side of the hole and from a crack at the neighboring hole, as far as applicable.

The growth of each initiated crack is estimated through the techniques of linear elastic fracture mechanics. Based on da/dn versus ΔK data suitable for the specific problem and material, the coefficients for the crack growth equations are determined. Two different crack growth equations are implemented in the computer code, i.e. the Forman and the Paris equation:

Paris equation: $$\frac{da}{dn} = C\,\Delta K^{n}$$

Forman equation: $$\frac{da}{dn} = \frac{c_f\,\Delta K^{n_f}}{(1-R)K_f - \Delta K}$$

There are different ways of calculating the stress intensity factor, e.g. FEM, BEM (Boundary Element Method), complex stress functions or compounding. Since a very important feature within a Monte-Carlo simulation is the computer time consumption, this model uses the compounding method, because it combines reasonable accuracy with very short calculation time compared to other methods.

The stress intensity factor is determined by a compounding process according to the formula proposed by Rooke et al. The process is simple and well known: known stress intensity factor solutions for simple configurations are combined to achieve results for complex configurations. Within this model a number of solutions account for the interaction of a crack with an object, where an object can be another crack, a hole, a boundary, etc. The resulting stress intensity factor K_r is then calculated by a summation procedure, where K_0 is the basic stress intensity factor without interaction, K_n is the stress intensity factor according to the interaction with one single object and K_e includes the influence of all objects together:

$$K_r = K_0 + \sum_{n\neq 0}(K'_n - K_0) + K_e$$

When calculating MSD scenarios it is essential to estimate the link-up process of these relatively small cracks. In the model two criteria have been checked which are:

- touching plastic zones proposed by Swift, which assumes that link-up of two cracks occurs when their plastic zones get in contact
- net section ligament failure, which assumes that link-up of two cracks occurs when the net stress in the remaining ligament exceeds the yield stress

Investigations and comparison with test results revealed that the Swift criterion may be not conservative in some cases, whereas the net section ligament failure criterion is in line with the test results.

2.5.3 Presentation of analysis results

The explained steps, determination of the initial damage scenario, damage accumulation and crack growth to a critical crack size, form a single Monte-Carlo iteration. From this iteration the Time to Initiation, the Time to Detectable and the Total Fatigue Endurance can be determined. During a complete Monte-Carlo simulation these steps are repeated n times. The results of n iterations are evaluated statistically to obtain probability distributions, mean values and standard deviation for the Time to Initiation, the Time to Detectable and the Total Fatigue Endurance. The final outputs of a complete Monte-Carlo simulation are crack and failure distributions associated with the multi-hole configuration specified. The results are generally presented graphically, e.g. the cumulative probability versus the number of cycles, as shown in the example in Figure 15.

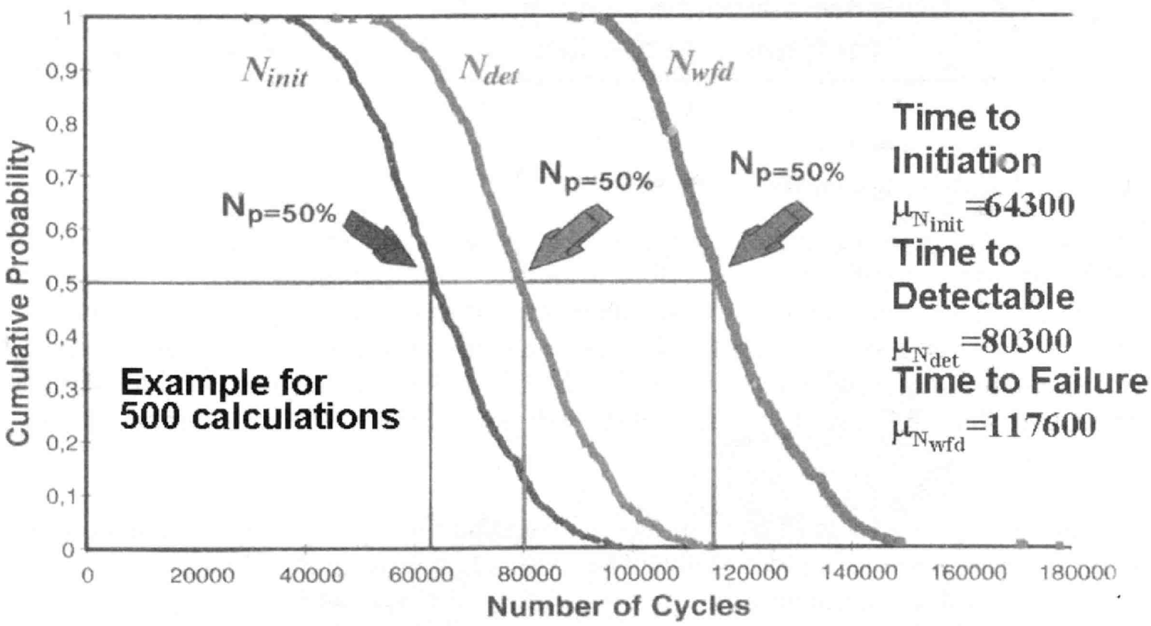

Figure 15: WFD analysis – presentation of results

3 FATIGUE TESTING

Airbus conducted for all new aircraft types sufficient structural tests for development purposes and to ensure that the in-service airplanes meet or exceed customer's requirements and expectations. A general overview about structural fatigue testing is shown in the test pyramid, see Figure 16. Development tests are accomplished to characterize the performance of new materials, validate new design and manufacturing procedures and demonstrate improved durability, safety and maintainability of the structure, as well as for definition of allowable stresses. Certification tests validate analysis methods and design allowables and lead to the final proof of structure.

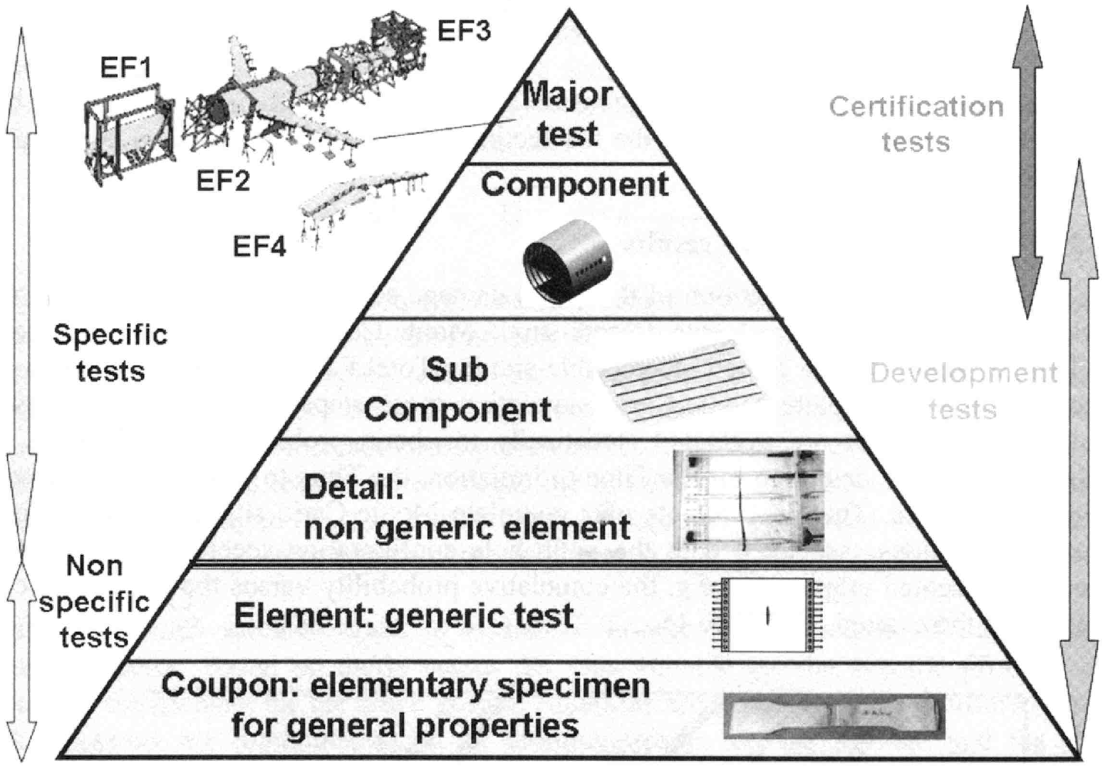

Figure 16: Test pyramid

3.1 Full scale fatigue tests

The damage tolerance regulations introduced in 1978 did not require full scale fatigue tests (FSFT) for type certification. Therefore American and European aircraft manufacturers developed different philosophies to validate their products. The European manufacturers, e.g. Airbus, considered FSFTs as certification tests and simulated minimum two life times. Since the introduction of Amendment 96 to FAR25.571 full scale fatigue tests are required to demonstrate that widespread fatigue damage will not occur within the design service goal of the airplane.

An overview about Airbus FSFTs and the achieved number of simulated flights is shown in Figure 17 from A300 to A340-500/600. The Airbus FSFTs were carried out as multi-section tests with the following test articles:

- EF1 – forward fuselage
- EF2 – center fuselage and wing
- EF3 – rear fuselage, including vertical tail plane, if metallic
- EF4 – horizontal tail plane
- EF5 – vertical tail plane, if composite

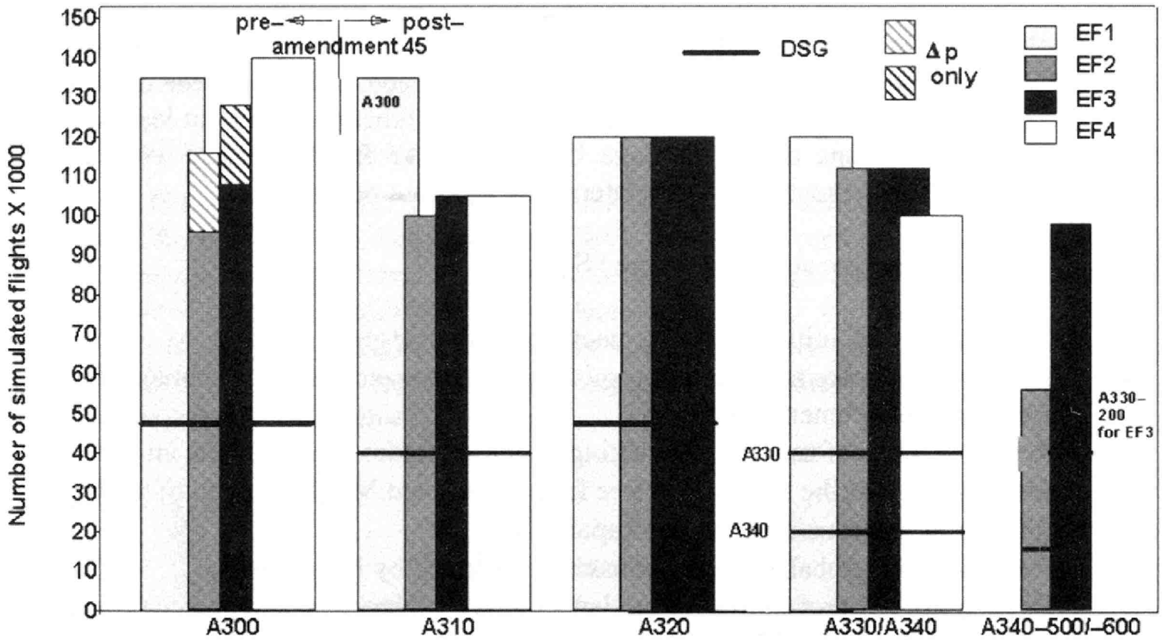

Figure 17: Overview of Airbus full scale fatigue tests

An example for a multi-section test is presented in Figure 18. This test procedure is applied to all Airbus aircraft from A300 to A340-600, i.e. over a period of approximately 30 years. The test philosophy of a multi-section test has significant technical, economic and temporal advantages, but needs a higher invest for the test equipment. All specimens of the multi-section test are tested simultaneously, but independently. This allows the simulation of an optimized test load spectrum for each individual test specimen by maintaining a common basic spectrum. Additionally this multi-section testing leads to a reduction in running time and inspection time compared with single-specimen testing. Due to the reduction of test time all test results are available significantly earlier and allow an early introduction of the repercussions in the production line, i.e. modifications.

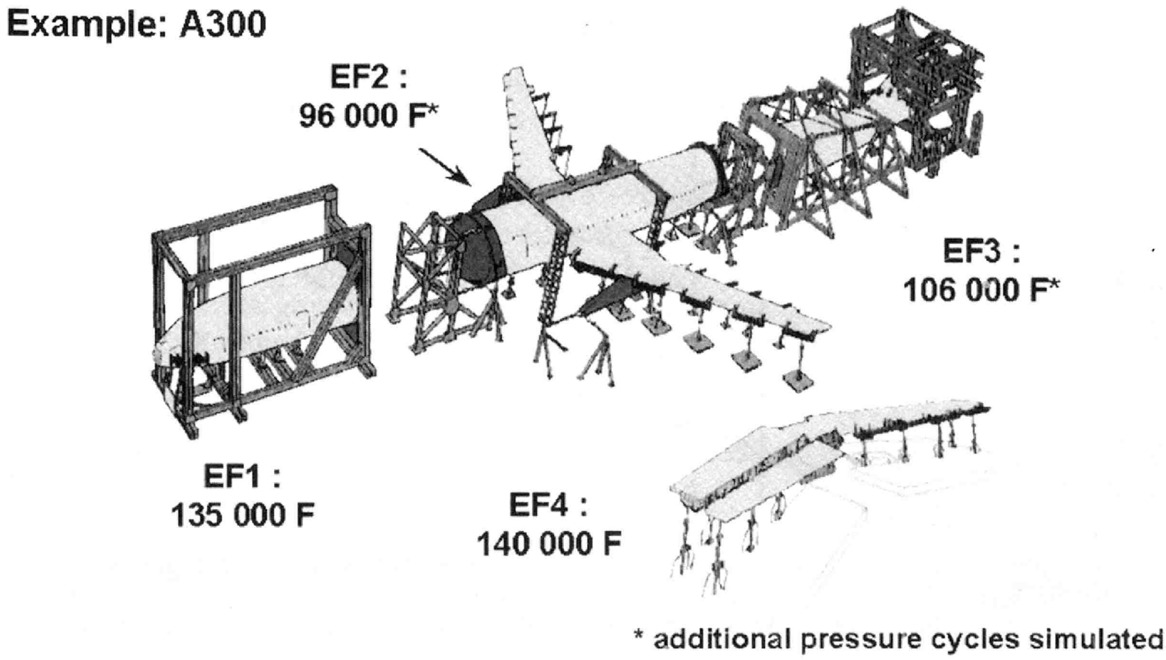

Figure 18: Example of multi-section full scale fatigue test

The multi-section test procedure described above is the favorite solution for all civil transport aircraft with a circular fuselage cross section. For the new Airbus product A380-800 a complete FSFT will be performed due to the oval fuselage shape. Splitting of the fuselage into several sections and attaching these sections to rigid steel bulkheads would not lead to correct stresses over large portions of the fuselage. Especially the frame stresses would not be reliable, since the displacements due to the lateral loads are not realistic.

There are several goals to be achieved by the FSFT such as:

- Validation of crack initiation life to meet the economic goals
- Validation of the predicted crack growth behavior to confirm the damage tolerance goals and the maintenance programs
- Detection of areas of early local cracking to change series production at an early stage
- Demonstration that the structure is free from significant MSD/MED up to the DSG
- Validation of the structural damage capability
- Validation of the global and local stresses determined by FEM analysis
- Validation of NDI procedures for hidden structure subject of maintenance program
- Validation of fatigue lives of repairs, reworks and dents to confirm repair concepts and allowable damages defined in the Structural Repair Manual (SRM)

The long term full scale fatigue testing allows the detection of nearly all significant areas which may be fatigue sensitive within the design service goal, since the scatter in loads and material data is covered sufficiently. The importance of this long term fatigue testing becomes obvious in Figure 19 which shows the development of the damages over the test progress for the EF2 specimens (center fuselage / wing). After simulation of one life time only 25 to 30 percent of all detected damages occurred at the A310 and A320 specimen; after two life times approximately 60 percent of the damages were detected. For the A330/A340 specimen the interpretation is more difficult, since the percentage of damages detected is related to the total number of damages after completion of the A330 testing. Furthermore at A330/A340 EF2 some early damages occurred due to the load program, which was very conservative for some areas.

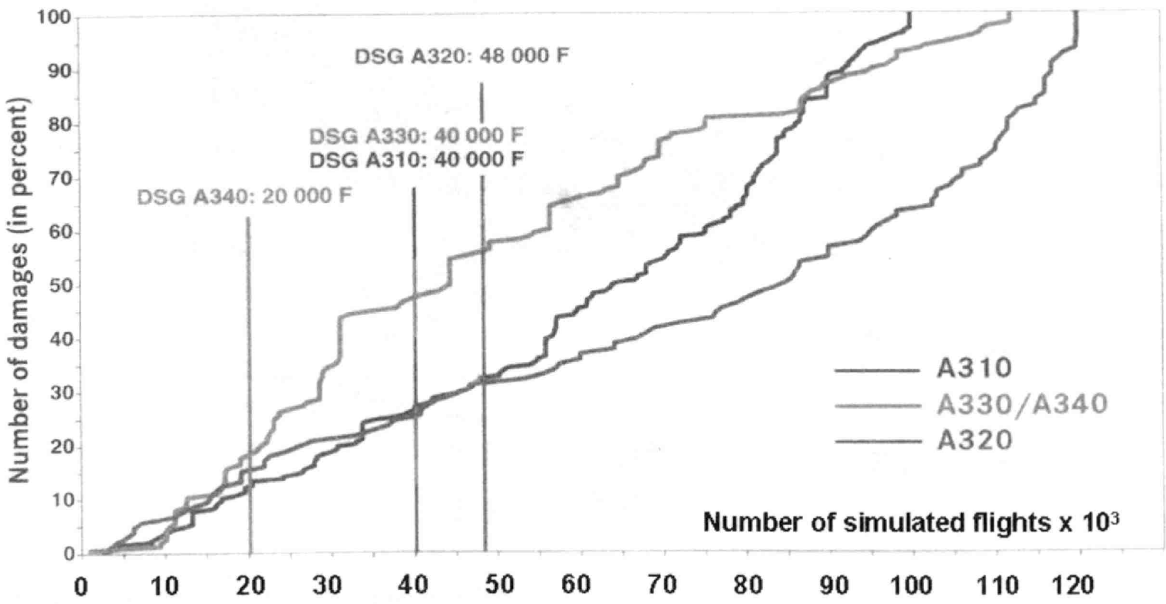

Figure 19: Development of damages during test progress – center fuselage / wing specimens

Besides full scale fatigue tests for certification large component tests are often performed for development purposes. Two examples of these tests performed by Airbus are presented in the following. Both specimens were tested under a complex flight-by-flight spectrum.

3.2 TANGO metallic fuselage barrel test

In frame of the research project TANGO (Technology Application to the Near-Term Business Goals and Objectives of the Aerospace Industry), which was partly funded by the European Union, a metallic fuselage barrel was tested, beside three other major component tests. The major objectives of the TANGO project were to improve the structural efficiency by reduction of the airframe weight and to reduce the manufacturing costs by using cheaper or more efficient materials and more efficient manufacturing technologies. Figure 20 shows an overview about the metallic fuselage barrel.

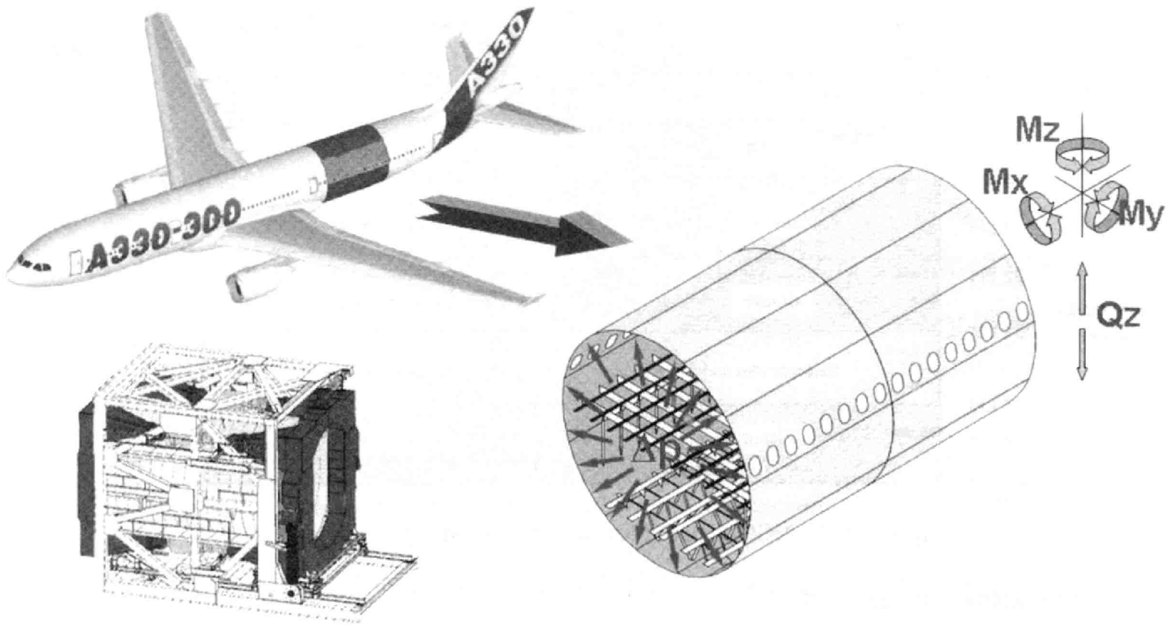

Figure 20: TANGO metallic fuselage barrel test

The design of the barrel panels is mainly concentrated on the fatigue and damage tolerance aspects. A summary of the design criteria is given in the following:

- Regulations FAR 25.571 Amendment 25-96 and AC 25.571-1C to be applied
- Fatigue and damage tolerance design criteria:
    - Fatigue design: no significant cracking before two times of A330 DSG
    - Crack growth: no critical crack growth during A330 inspection intervals
    - Residual strength: two-bay-crack criterion to be met
    - Widespread fatigue damage: no occurrence prior to two times of A330 DSG
- Static design criteria:
    - Maximum load: 1.5 times of once per life fatigue load or 1.1 times limit load *
- Design for reparability

The reduced loading for the static design (*) is only applicable for the barrel. The reason for this decision is to reach high operational stresses in large areas of the barrel specimen to validate the increased allowable stresses for the new technologies.

All of the three research partners (Alenia, SAAB, Airbus Germany), which participated at the metallic fuselage barrel, provided panels of various technologies. GLARE® panels were mainly be located in the upper fuselage area where the advantages of GLARE® may be exploited. Panels with advanced bonding technologies were located in the side shells to evaluate their capability regarding shear stresses. Furthermore manufacturing costs may be reduced by avoiding the riveting of the window frames. Welding technologies were applied mainly to panels in the lower fuselage area. Figure 21 shows the panel arrangement including the partners´ contributions.

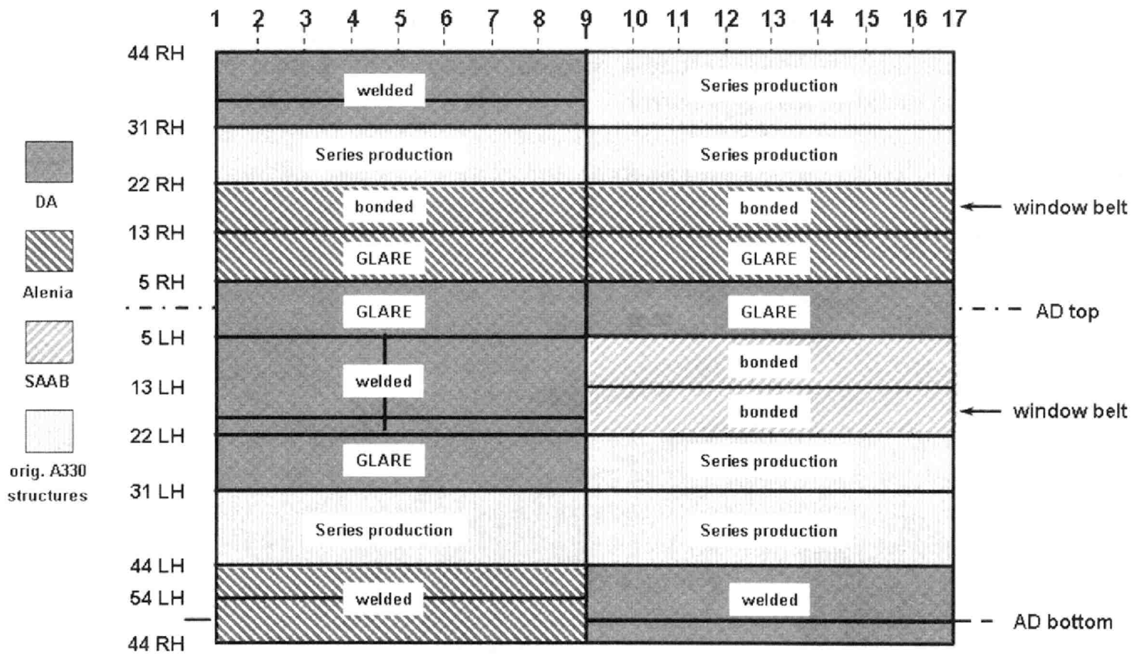

Figure 21: TANGO metallic fuselage barrel test – panel arrangement

3.3 Megaliner barrel test

The most important test for development of a large aircraft with an oval fuselage cross section is the so-called Megaliner Barrel test, see Figure 22.

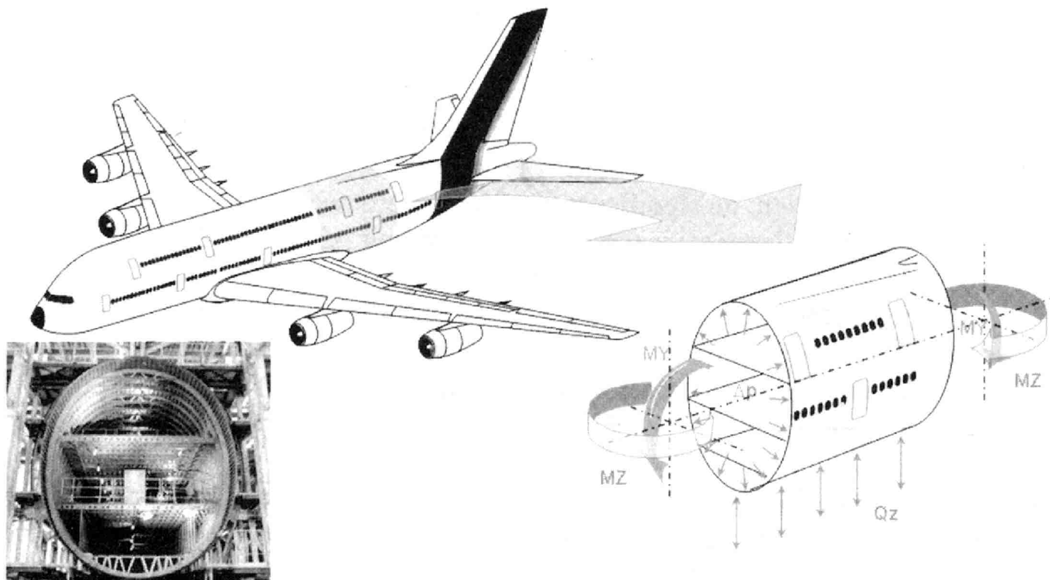

Figure 22: Megaliner barrel test

This test was partly funded by the German government. Figure 22 shows an overview of the test article, the fuselage area represented and the loading of the barrel. Major features of this test are the two passenger decks, two rows of windows, the door cut-outs, a slide raft cut-out, the floor support beams and the truss structure. The major objective of the Megaliner barrel test was to support the material and technology development of metallic and fiber metal laminate fuselage structures for large fuselages with a non-circular cross section. Figure 23 shows the panel arrangement at the test specimen.

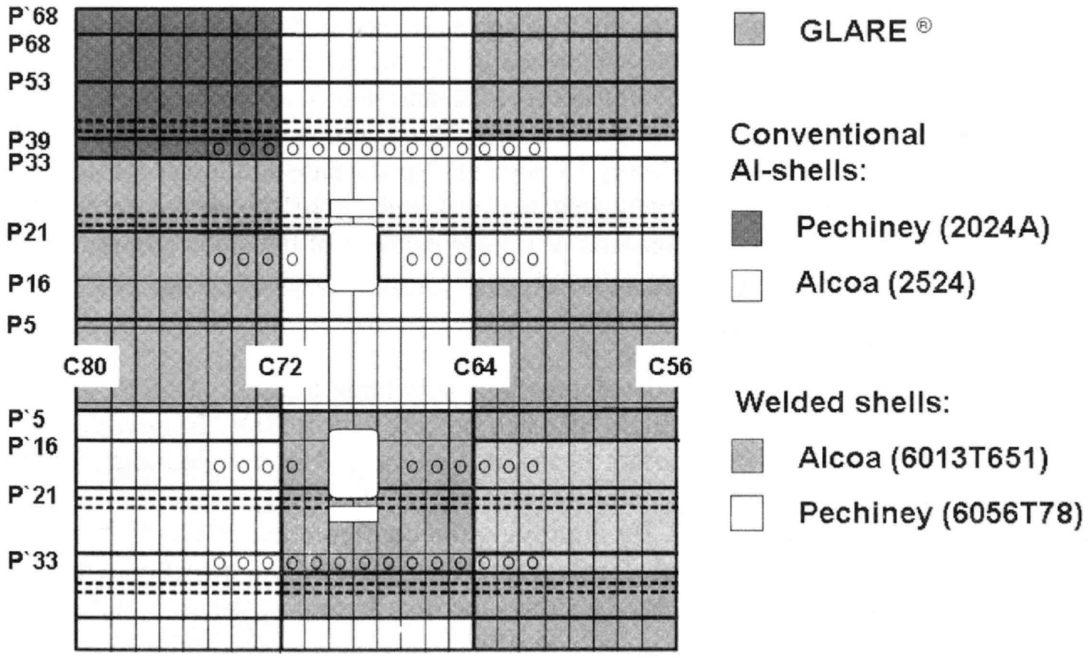

Figure 23: Megaliner barrel test - panel arrangement

4 DEVELOPMENT OF ADVANCED METALLIC FUSELAGE STRUCTURE

During the last years significant improvements have been achieved for fuselage structures by using new design principles, advanced materials and improved manufacturing processes. However; there are still ongoing activities for further developments. Four key airframe drivers are identified which include the following primary objectives:

1. Development: low weight structure, low non-recurring costs, high performance aircraft, reduced design times
2. Manufacturing: low recurring costs, short flow time, reduced impact on environment,
3. Operation: increased safety and reliability, reduced inspections and improved reparability, low operating costs, low environmental impact (emissions and noise), increased operational capacity and passenger comfort
4. Disposal: possibilities of recycling, low environmental impact

The major developments discussed in this paper are: advanced materials, fiber metal laminates (GLARE®), laser beam welding, friction stir welding, bonding / metal laminates and structural health monitoring.

4.1 Advanced materials

During the initial design phase of new aircraft types the application of new materials and production methods is considered to reduce the production costs and the structural weight as well as to comply with the new regulations. The fuselage skins of all Airbus aircraft certified up to 2001 were made of 2024T3, T42 or T351. The stringer material was 2024T3 in the upper shell and 7075T73 in the lower shell, which is mainly designed by compression loads.

The first step to apply new materials for the fuselage skin was made for the derivatives of the A340, i.e. for the A340-500 and –600, which are stretched versions of the basic A340-300 and which have been certified in 2002. For the forward and rear fuselage the material 2524T3 has been selected for the skin in the upper shell, which allows increasing the allowable longitudinal skin stresses by approximately 15 percent. For the side and lower shells the basic 2024 material is kept except in a small area forward and aft of the center section where 7475T761 was selected due to static reasons. For improvement of the static strength stringers of high strength material 7349T7 were selected for the whole fuselage circumference with a few exceptions.

An additional challenge exists for the development of very large transport aircraft, e.g. Airbus A380, which recently made the first flight and will be certified in 2006. In theory, when the size of an aircraft is increased by a certain factor, its volume and its weight increase with the factor to the third power. This exponential increase means that weight aspects of very large transport aircraft are quite significant. By improving the configuration of these aircraft types, the effect of this law can be reduced. Furthermore new materials and technologies play a major role for very large aircraft. Figure 24 shows the distribution of the skin material at the Airbus A380-800.

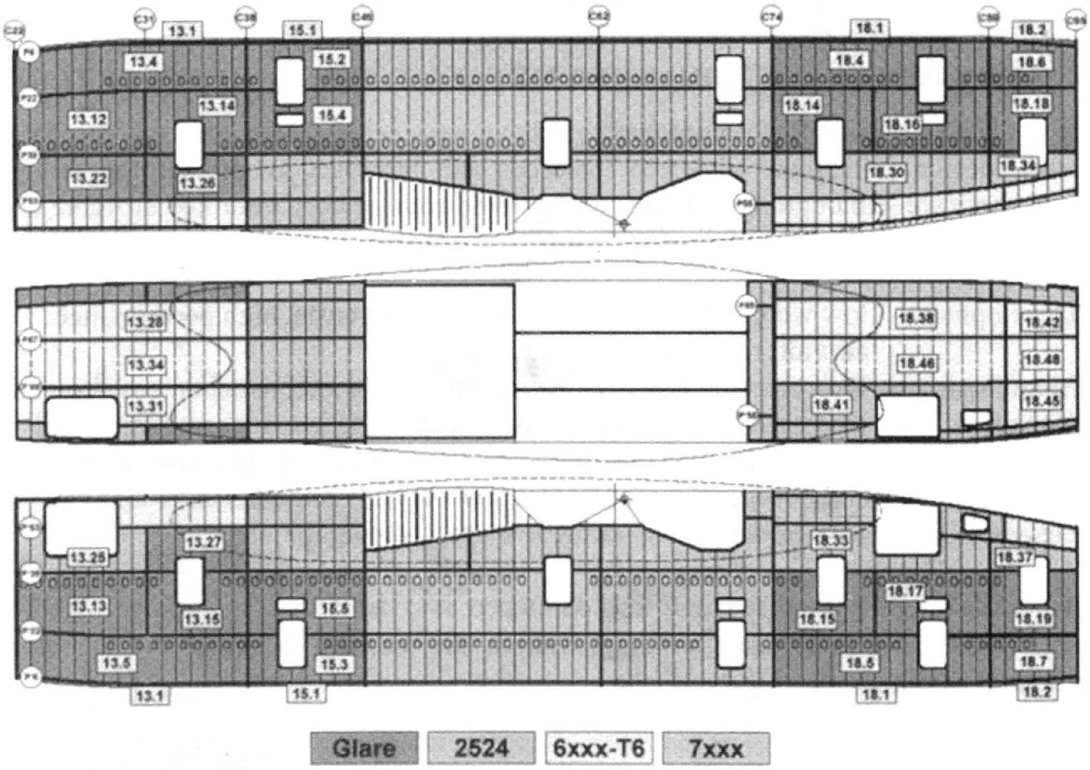

Figure 24: Airbus A380-800 fuselage skin materials

In addition to the materials for A380-800, which are qualified or under qualification, further materials are under development for future application in fuselage skins, e.g. the Al-Li alloy C47A T8 from ALCOA and the AlMgSc alloy Ko8242 from CORUS with the following characteristics:

- Al-Li C47A T8:
  - third generation alloy (Li content <2%)
  - Optimized thermal treatment for improved stability
  - High static and fatigue properties, and excellent crack propagation behavior
- AlMgSc Ko82842:
  - High damage tolerance properties
  - High thermal stability (creep forming possible)
  - High corrosion resistance

Both alloys are weldable and show a good corrosion resistance, i.e. cladding is not necessary. Table 1 shows the relative improvements compared to 2524.

	Comparison vs. 2524 T351	
	Al-Li C47AT8	AlMgSc Ko8242
Density	- 5.1 %	- 4.7 %
Young´s modulus	+ 7 %	+ 4 %
Yield strength (L / LT)	+ 11% / + 20 %	-13 % / 0 %

Table 1: New Al alloys in comparison with 2524 - examples

4.2 Fiber metal laminate GLARE®

Fiber metal laminates (FML) were developed at Delft University of Technology as a family of new hybrid materials consisting of bonded thin metal sheets and fiber/adhesive layers. The laminated structure provides materials with excellent fatigue, impact and damage tolerance characteristics at low density. The trademarks are ARALL® and GLARE®. The prepregs act as barriers against corrosion and the laminate has an inherent high burn-through resistance as well as good damping and insulation properties. GLARE® provides an attractive weight saving potential of approximately 10 to 20 percent for fuselage panels dimensioned by damage tolerance behavior. The higher value may be achieved only, if the stringers are made of GLARE® too. The material provides several improvements such as low density, high durability, slow crack growth, high residual strength, high corrosion resistance and high fire resistance. GLARE® is a hybrid material built-up from alternating layers of aluminum sheets (thickness between 0.2 and 0.5 mm, mainly made from 2024T3) and glass fiber reinforced adhesive unidirectional layers (FM94-S2-Glass, thickness 0.125 mm). Figure 25 shows the general definition of GLARE® and Table 2 contains the eight standard GLARE® types.

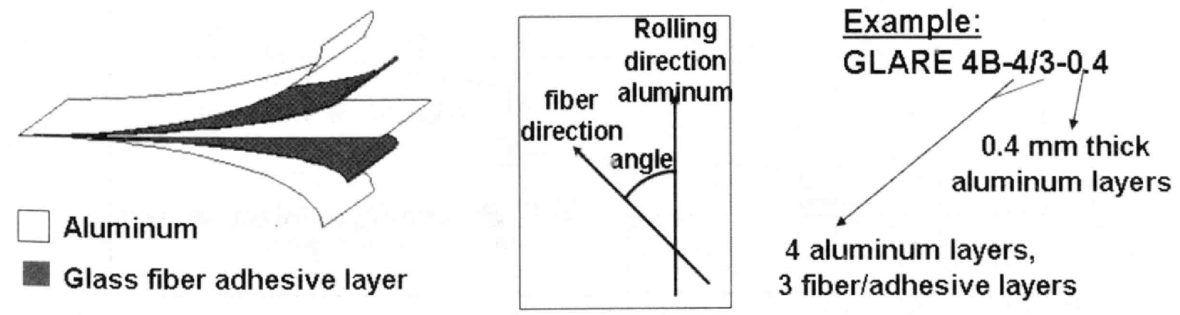

Figure 25: Definition of GLARE®

Standard GLARE® types	Fiber adhesive layer (mm)	Fiber/adhesive layer built-up	Al alloy
GLARE 1	0.25	0°/0°	7475T761
GLARE 2A	0.25	0°/0°	2024T3
GLARE 2B	0.25	90° / 90°	2024T3
GLARE 3	0.25	0° / 90°	2024T3
GLARE 4A	0.375	0°/90°/0°	2024T3
GLARE 4B	0.375	90°/0°/90°	2024T3
GLARE 5	0.5	0°/90°/90°/0°	2024T3
GLARE 6	0.25	+45°/-45°	2024T3

Table 2: Standard GLARE® types

The crack growth behavior of GLARE® has been investigated in several curved panel tests such as shown in Figure 8 LH. The crack growth behavior of the longitudinal cracks between intact frames in GLARE4B is presented in Figure 26 in comparison to other materials [16]. The panels have a radius of 2820 mm and the maximum internal pressure during test was 593 hPa. The initial crack lengths for these tests vary between 75 mm and 100 mm.

The crack growth periods for panels made of 6013T6 or 2024T3 with a thickness of 1.6 mm are nearly identical from an initial crack of 75 mm. A material change to 2524T3 and an increase of the skin thickness to 1.8 mm improves the crack growth period by approximately a factor of 3. A much more superior behavior shows the material GLARE4B, which was tested with a skin thickness of 1.95 mm. Up to a crack length of approximately 200 mm the crack growth was very slow. To accelerate the test the intact fibers, which provide a bridging of the crack in the metal were cut several times. After a crack length of 250 mm was reached the crack growth increased a bit. The crack growth period up to the test stop, where the crack growth rate was still quite moderate, is significantly greater than for the conventional 2024T3 material. However, the results are not directly comparable, since, on one hand, the 2024 skin was thinner than the GLARE4B skin and, on the other hand, the fibers of the GLARE4B material were cut four times which is no natural damage scenario.

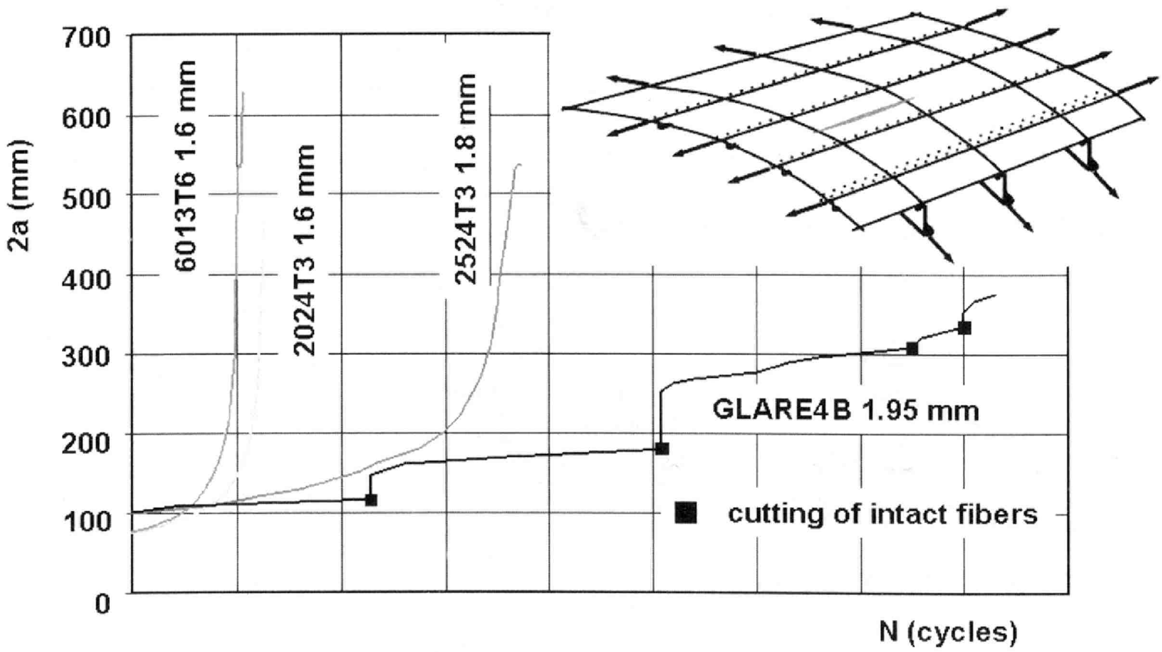

Figure 26: Crack growth behavior of longitudinal skin cracks between intact frames in GLARE®

GLARE® offers an excellent crack growth behavior for both crack types, i.e. for the so-called through cracks and part-through cracks. This superior behavior is the result of the presence of fibers in the laminate [17], which do not fail due to fatigue. This enables load transfer over the crack through the fibers, thus reducing the crack tip opening, the stress intensity factor and finally the crack growth rate. Figure 27 shows the crack bridging of the fibers. Although the stresses in the aluminum layers are higher than the stress applied to the laminate, the crack propagation period is much longer due to the crack bridging effect explained above. This is due to the low stress intensity factor when the crack reaches a certain length and the fibers become effective.

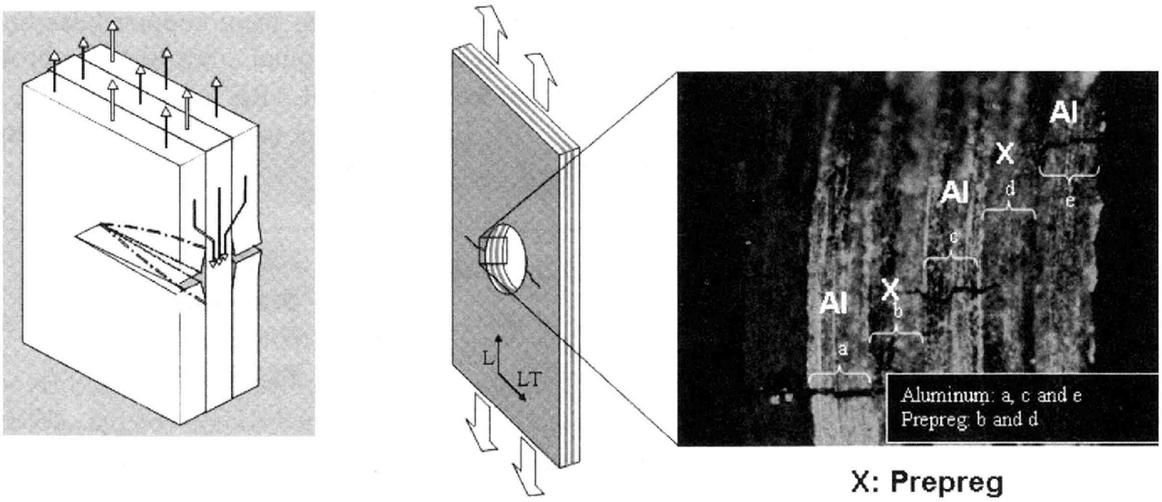

Figure 27: Bridging effect of GLARE®

The fatigue and damage tolerance analysis of GLARE® structure is performed according to the definitions given in Table 3. Fatigue initiation mainly affects the aluminum layers in GLARE®, i.e. the fatigue initiation process is similar to that of monolithic aluminum. Similar stress level and stress concentration in the aluminum leads to the same time to crack initiation. A fatigue initiation in Glare is calculated in the same way as for monolithic aluminum by using the actual stresses in the aluminum layer at critical location. The actual stresses in the aluminum layers in Glare consist of stresses due to curing process, external loads and temperature deviating from ambient conditions. The crack growth analysis may as well be based on metal methods. Since the residual strength analysis needs to assume aluminium layers and fibers to be broken, special methods were developed at the Technical University of Delft.

Analysis	GLARE® phenomena	Methods applied	
Crack initiation and crack growth	Cracks in metal layers only, fibers remain intact	Treat GLARE® as a metal	Metal methods for initiation [18]
			Metal methods for crack growth [18]
Residual strength	Final failure in complete sheet, therefore failure in both, aluminum and fibers	Apply dedicated methods for GLARE®	Crack with fibers broken: R curve concept [19]
			Crack(s) with fibers intact: Reduced Blunt Notch Strength Method [20]

Table 3: Analysis methods for GLARE® structure

Recently a further development of GLARE® was initiated in order to reach an optimized balance of the structural properties of GLARE®, which is called HSS (High Static Strength) GLARE. It has been developed as a member of the FML family with increased static properties compared with the first variant (called "Standard GLARE®"). This has been achieved by using a 7475-T761 aluminum foils instead of 2024-T3. The main improvements are found in shear properties and yield strength. Because of the high fatigue allowables for Glare, large parts of the A380 fuselage are statically dimensioned. For these panels, additional weight saving opportunities are provided by HSS GLARE®.

Tests have been performed to investigate HSS GLARE®, ranging from coupon tests up to large curved stiffened shells. Crack propagation tests of a longitudinal crack above a broken frame showed a minor increase of da/dN compared to Standard GLARE®, see Figure 28, but still significantly lower than in monolithic Al 2524. Large damage capability was proven at 1.15 times Δp for a two-bay-crack over a broken frame.

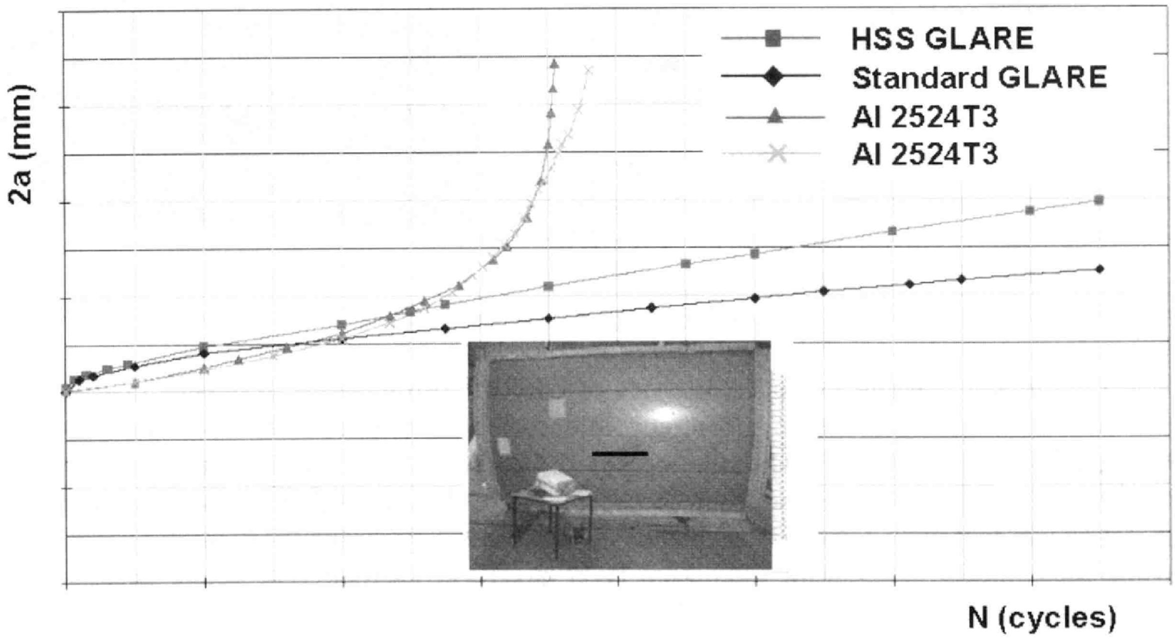

Figure 28: Crack growth behavior of HSS GLARE®– longitudinal crack above broken frame

Another beneficial feature of GLARE® is the capability to provide an excellent structural damage capability. This results firstly from the excellent damage tolerance behavior of GLARE®, which is described above. Furthermore GLARE® provides the opportunity to initiate a crack turning, e.g. the crack turning of a long crack at the adjacent frames, which prevents explosive decompression of the fuselage. The crack turning effect is reached by embedding additional glass fiber layers in the material at the frame locations, see Figure 29.

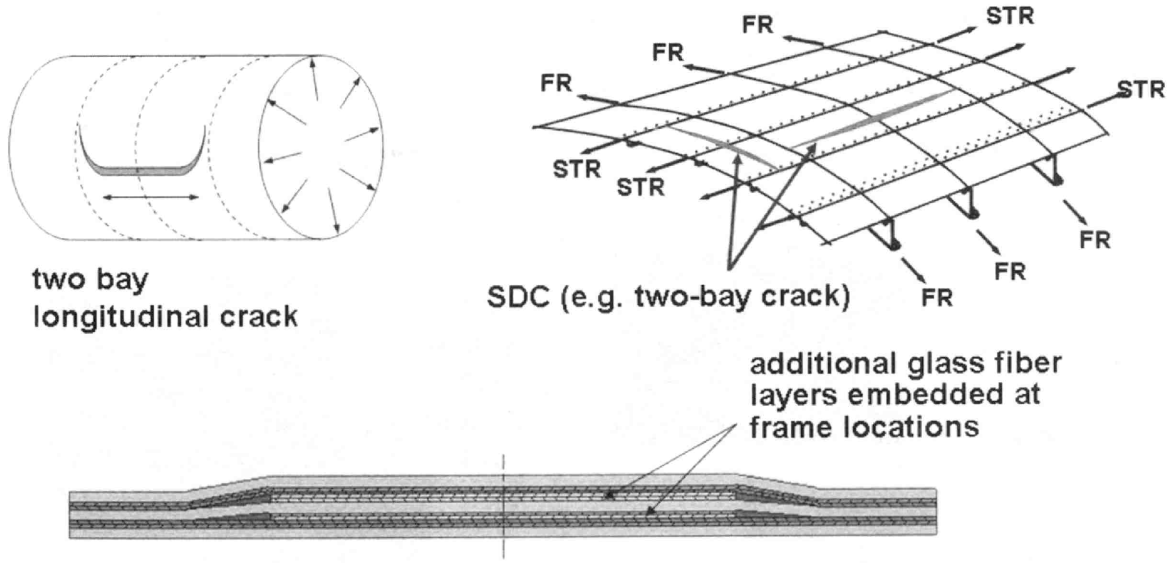

Figure 29: Structural damage capability provided by GLARE®

4.3 Welding technologies

For Airbus fuselages two welding technologies are under consideration: Laser Beam Welding (LBW), already applied in series production, and Friction Stir Welding (FSW), still under investigations, see Figure 30. Welding technologies are mainly introduced to reduce the manufacturing costs. A weight saving may be reached in addition.

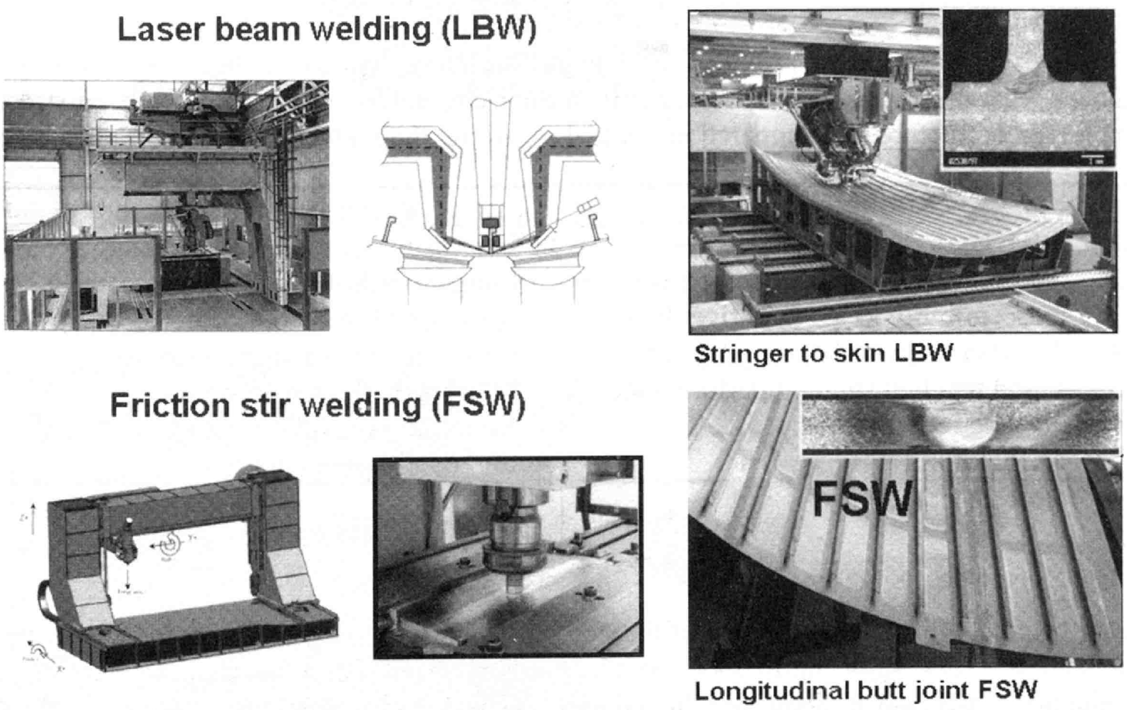

Figure 30: Welding technologies

The application of welding technologies will change the design philosophy for the fuselage panels, e.g. when welding stiffeners to the skin. Since recently pressurized fuselages of commercial transport airplanes generally consist of a built-up structure where the skin-to-stringer connection may be riveted or bonded. The other connections such as skin-clip (shear ties) and clip-frames are riveted, see Figure 31. The materials used are in general the aluminum 2000 series (2024, 2524) for all elements. In specific areas 7000 series alloys (7475, 7075, 7349) are used to increase the static strength and/or the residual strength.

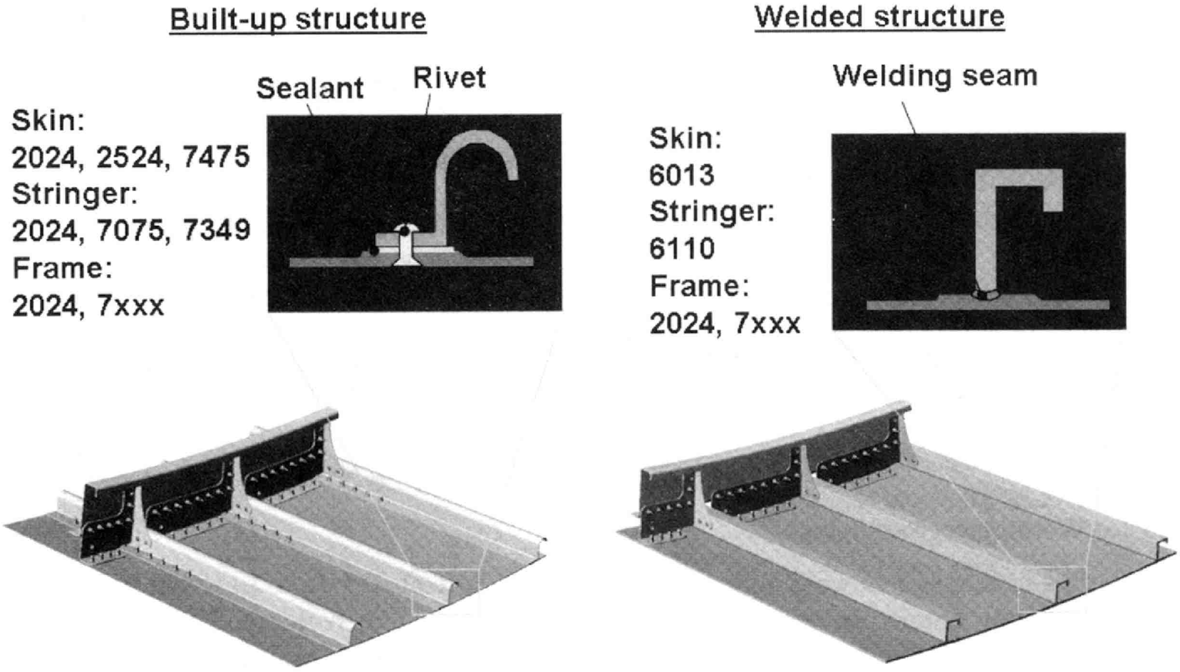

Figure 31: Built-up structure versus integral (welded) structure

Welding of the stringers provides an integral structure, which changes significantly the damage tolerance behavior of the panel regarding circumferential cracks. Built-up structure and integral structure are compared in Table 4 regarding their advantages and disadvantages.

	Built-up structure	Integral (welded) structure
1.	Riveting is slow and expensive	Fast manufacturing (cost savings)
2.	Shorter crack free life (durability)	Longer crack free life
3.	Susceptibility to MSD in rivet line	No susceptibility to MSD
4.	Good crack retardation capability	Low crack retardation capability
5.	Good residual strength performance	Low residual strength performance
6.	Sealing required	No sealing required (cost saving)
7.	Difficult inspectability	Improved inspectability

Table 4: Comparison of built-up structure and integral structure

4.3.1 Laser beam welding

Laser beam welding (LBW) is one of the most promising welding technologies for aerospace application. The major motivation of the application of LBW is the reduction of the production costs and a slight weight reduction. The LBW technology is most suitable for welding of T-joints, e.g. skin-to-stringer or skin-to-clip joints. Weldable aluminum alloys such as 6013 and 6056 have to be used for the time being.

One of the first applications of LBW on primary structure of a commercial transport airplane are the lower and side shells of the Airbus A318 using 6013 and 6056 for skin to stringer welding, see Figure 32. Furthermore lower and side shells of the A380-800 are welded (skin-stringer joint) as well as a forward bulkhead panel. Also several panels of a high gross weight version of the A340 are welded. However, to date an application of the welded structure in all areas of the pressurized fuselage is not appropriate due to the limited residual strength capability of the integral structure. In the welded areas of the A318 and A380-800 the operational tension stresses (in stringer direction) are rather low, since the lower and side shells are dimensioned mainly by compression.

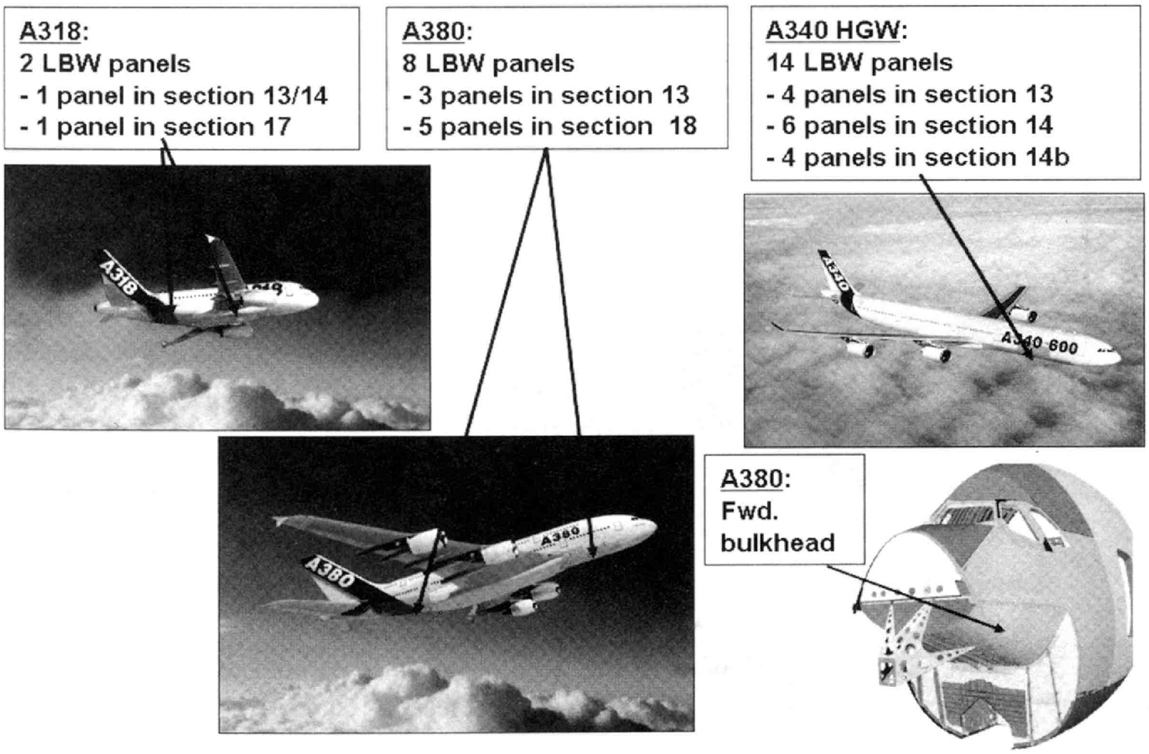

Figure 32: Application of LBW at Airbus aircraft

Further development is performed for welding of other structural parts, e.g. the welding of the shear clips to the skin. This is an additional challenge, because there is no continuous weld line over several meters, i.e. the weld line is interrupted approximately every 150 mm, see Figure 33.

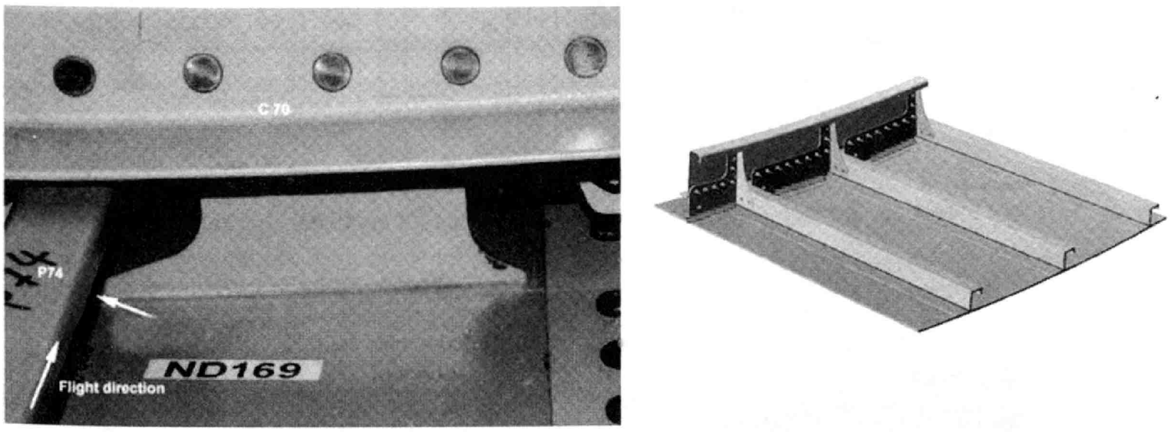

Figure 33: Laser beam welding of shear clips to skin

The fatigue behavior of welded joints, i.e. the life to crack initiation has been checked for both, transverse and longitudinal direction, i.e. loading perpendicular and parallel to the weld line [21]. Figure 34 shows the fatigue behavior of the welded structure transverse to the weld line. The welded joint shows fatigue lives comparable to a K_t = 3.6 specimen. The actual aircraft stress level is significantly below these SN- curves.

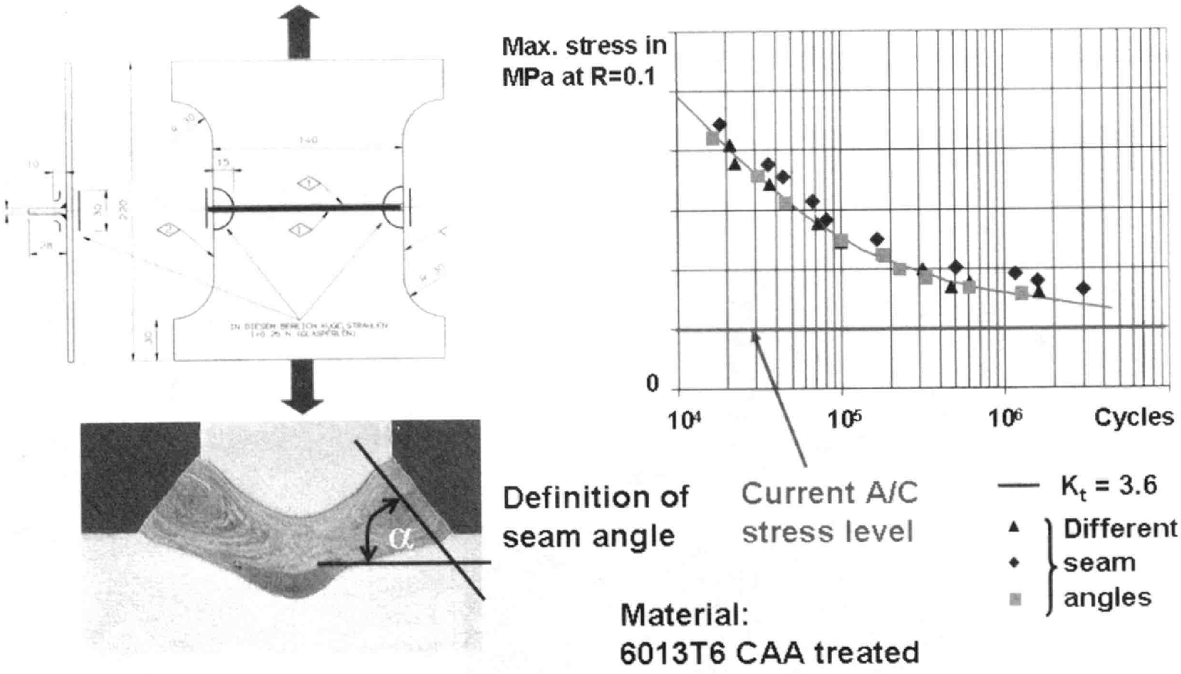

Figure 34: Fatigue behavior (transverse) of laser beam welded skin stringer joint

Figure 35 shows the fatigue behavior of the welded structure parallel to the weld line. The actual aircraft stress level is again significantly below these SN- curves.

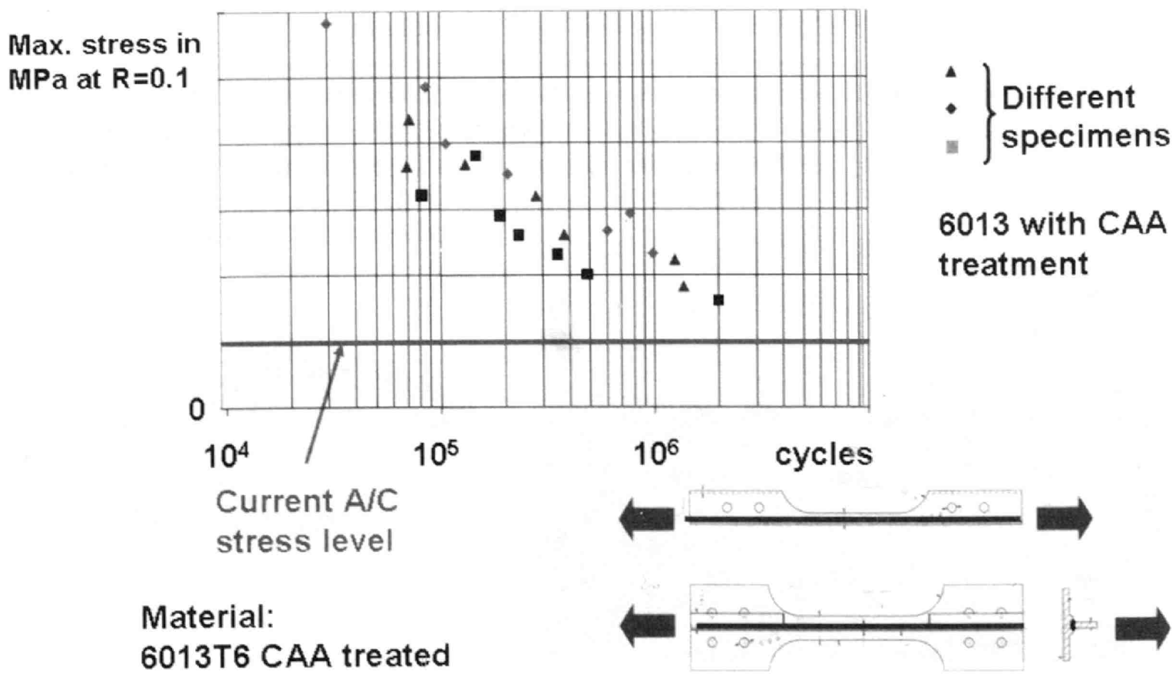

Figure 35: Fatigue behavior (longitudinal) of laser beam welded skin stringer joint

The damage tolerance behavior of the welded structure is mainly influenced by the type of structure, i.e. integral structure, and only secondarily by the material [22]. As explained above integral (welded) structure provides only limited retardation of cracks and reduces the residual strength significantly, since the crack propagates simultaneously in the skin and the stringer, as demonstrated in Figure 36.

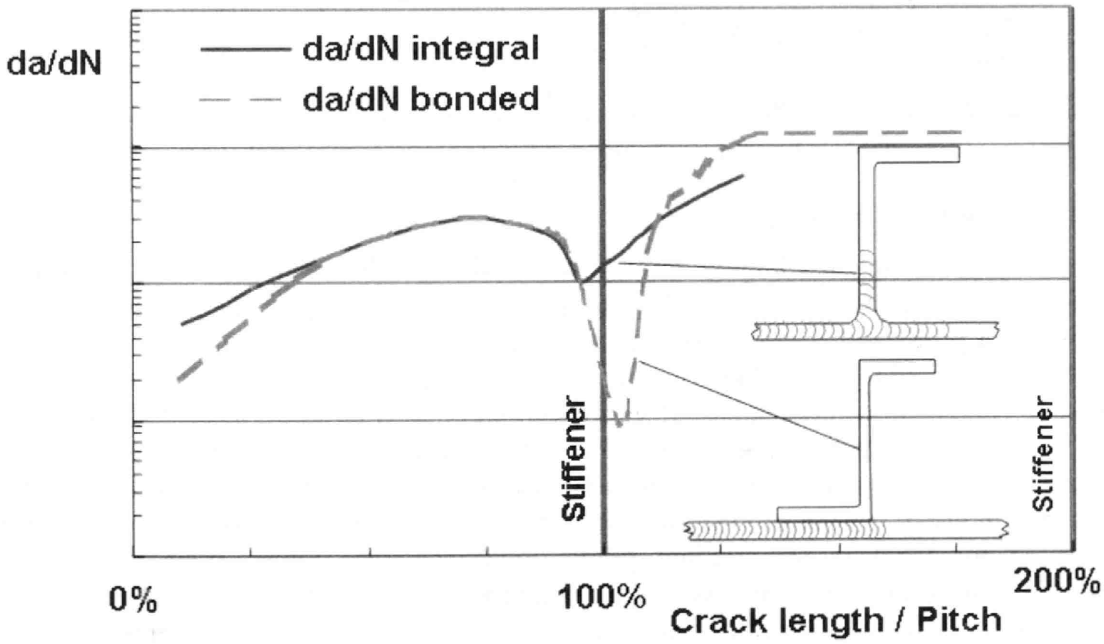

Figure 36: Crack growth behavior of circumferential cracks in integral and built-up structure

Table 5 shows the allowable stresses for crack growth and residual strength in panels containing a circumferential crack. The allowable stresses are determined to reach a pre-defined inspection interval and to sustain a two-stringer-bay crack above a broken stringer. The values show significant differences between built-up and integral structure. Furthermore the advantages of bonded stringers compared to riveted stringers are obvious.

Assembly of stringers (Materials skin + stringer)	Allowable stress for circumferential crack	
	Crack propagation	Residual strength
Riveted (2524+7349)	100 %	100 %
Bonded (2524+7349)	115 %	110 %
Welded (6013HDT-T6)	85 %	65 %

Table 5: Allowable stresses for circumferential crack above broken stringer in skin panel

The damage tolerance behavior of longitudinal cracks was also investigated in [22]. The allowable stresses in the skin containing a longitudinal crack above a broken frame are independent of the connection of the stringers (riveted, bonded or welded). Therefore the allowable stresses dependent only on the material, provided the crack is not assumed in the rivet / bond /weld line, and results in the same value for 2425 and 6013HDT-T6.

The residual strength behavior is investigated assuming a crack in the rivet /weld line compared to the base material, see Table 6. According to the investigations performed up to now the thermo-mechanically affected zone (TMAZ) is the worst area in a friction stir welded joint. The fracture toughness of the LBW skin – stringer joint in the transition between the weld zone and the basic material shows approximately the same K_{C0} value in tests performed at room temperature. At -30°C the fracture toughness drops by approximately 15 percent.

Material / Technology	K_{C0} (MPa$\sqrt{m}$)
FSW skin butt joint, 6013T6, TMAZ	100
LBW skin - stringer joint, 6013T6, transition weld zone – basic material	99
LBW skin - stringer joint, 6013T6, T = -30°C, weld zone – basic mat.	84
Riveted skin - stringer joint, 2524T3, rivet line	111
6013T6 base material	127
2524T3 base material	143

Table 6: Fracture toughness of skin panel (crack in rivet / weld line)

4.3.2 Friction stir welding

The second promising welding technology is the friction stir welding (FSW), which is based on patents developed by the "The Welding Institute" (TWI) in UK. The process consists of a rotating tool producing frictional heat so that plasticized material in kneaded under pressure and therefore leading to a tight connection of the sheets. FSW allows joining of "non weldable" alloys, e.g. 2000 and 7000 series aluminum alloys. Furthermore different materials may be joined, e.g. different Al alloys. For series production FSW is today applied in non-aircraft industry. Examples for application are ship and train manufacturing as well as aerospace industry (rocket production). In the aircraft industry first applications of FSW are envisaged for fuselage longitudinal joints, wing spanwise joints, wing spars made of dissimilar alloys and extruded panels, e.g. in center wing box. FSW is a welding technology, which offers a lot of opportunities. The most important aspects are summarized in the following. These aspects offer either (1) a design improvement or (2) manufacturing savings or both.

- Fastener reduction (1), (2)
  - No fatigue cracking at fasteners holes (no MSD)
  - Reduced manufacturing costs
  - No sealing
  - Typical application: fuselage longitudinal joints, wing spanwise joints
- Material optimization (1)
  - Weld "non weldable" aluminum alloy (e.g. 2024 and 7075) and dissimilar alloys (2024-6013 or 7075-8090)
  - Envisaged application: Spars from different alloys
- Material utilization (2)
  - Reduce the buy to fly ratio by welding machining blanks
  - Reduce the constraint of material supplier maximum workable volume
  - Typical application: wing ribs and wing spars
- Process automation (2)

Figure 37 shows the different zones, which are created during the friction stir welding. These zones have different properties, e.g. hardness, fatigue initiation, crack growth and residual strength behavior. Therefore the relevant properties for dimensioning the joint have to be checked in each of the zones.

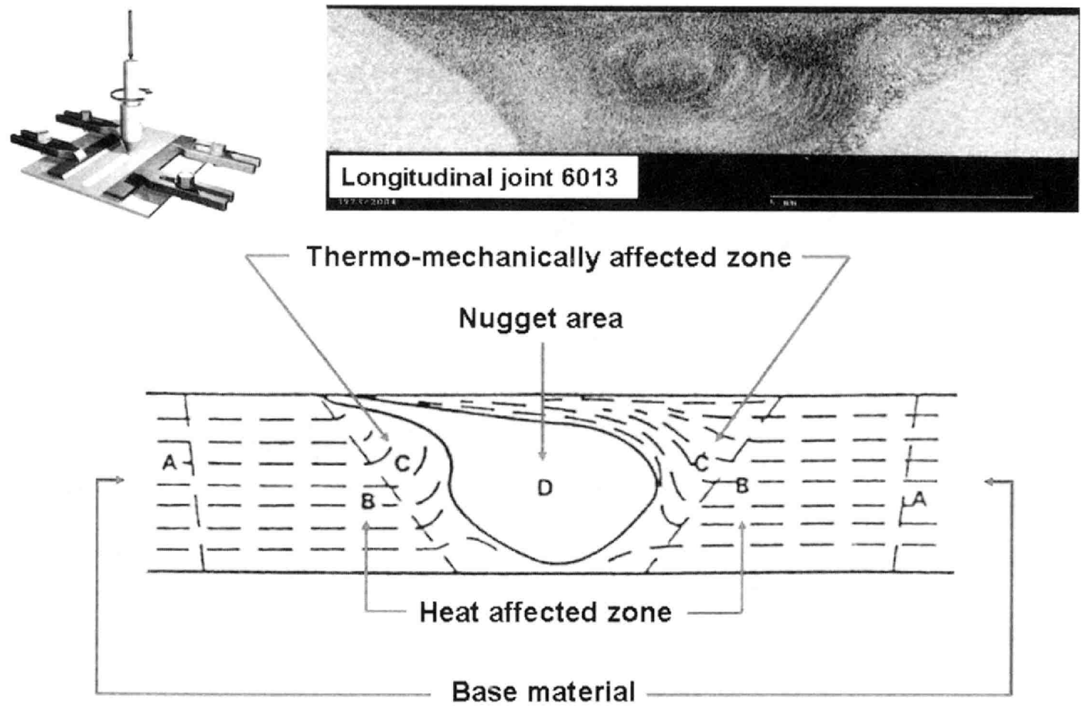

Figure 37: Zones in area of friction stir welding

The static properties of FSW joints are excellent compared to the base material, see Table 7 for several materials and a thickness range around 4 mm.

Material	Static properties of FSW butt joints
2xxx	Very high – 90% of base material
6xxx	High – 80% of base material
7xxx	High – 80% of base material
AlMgSc	Very high – 95% of base material
AlLi	High – 80% of base material

Table 7: Static properties of FSW joints

Figure 38 shows the excellent fatigue behavior of FSW joints compared to a riveted joint. The Figure contains the allowable stresses for an optimized three-rivet-row lap joint with additional doublers in the rivet area and three rivet rows, a three-rivet-row lap joint without doublers, and a FSW joint compared with the behavior of the baseline material. The allowable maximum fatigue stress (far field stress) is 54 percent lower for the riveted lap joint compared to the FSW joint. These figures are valid for specimens with a mean fatigue life of 250 000 cycles at an R value of 0.1.

The first very promising results of the crack growth and residual strength behavior of FSW joints in 6013T6 have been published in 2001 [23]. Further investigations confirmed these results, also for other materials. Figure 39 shows the da/dn vs. ΔK data and the R-curves for FSW joints in 6013 T6, AlMgSc and AlLi 1424Tx in comparison to the so-called 2024 master curve. The da/dn data and the R-curves show considerable differences depending on the zone of the weld line. The nugget zone provides the better results for most of the cases investigated. The da/dn data are better or equal compared to the 2024 master curve

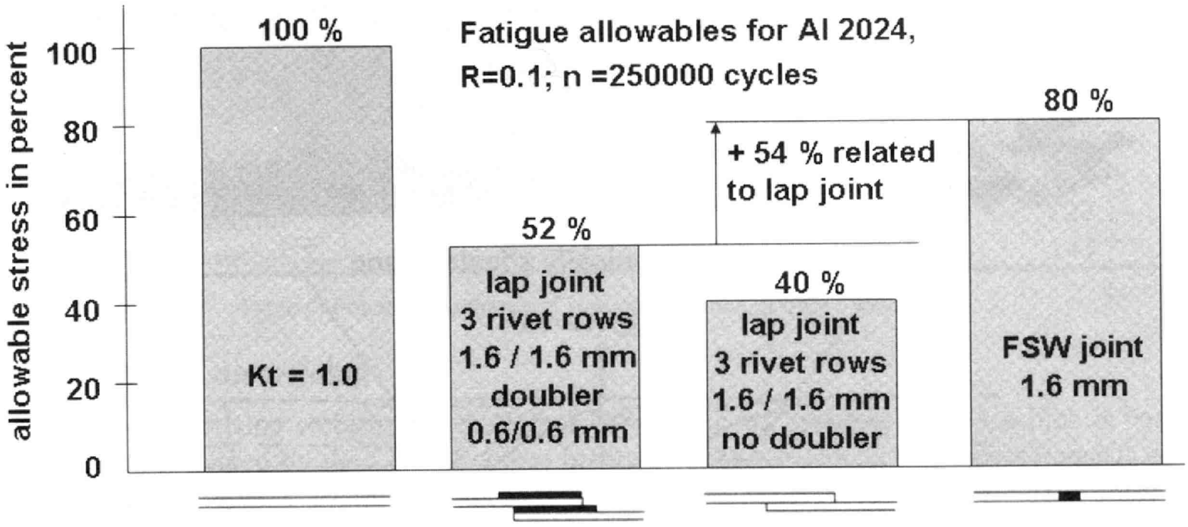

Figure 38: Fatigue life of FSW joint in comparison to riveted lap joint and base material

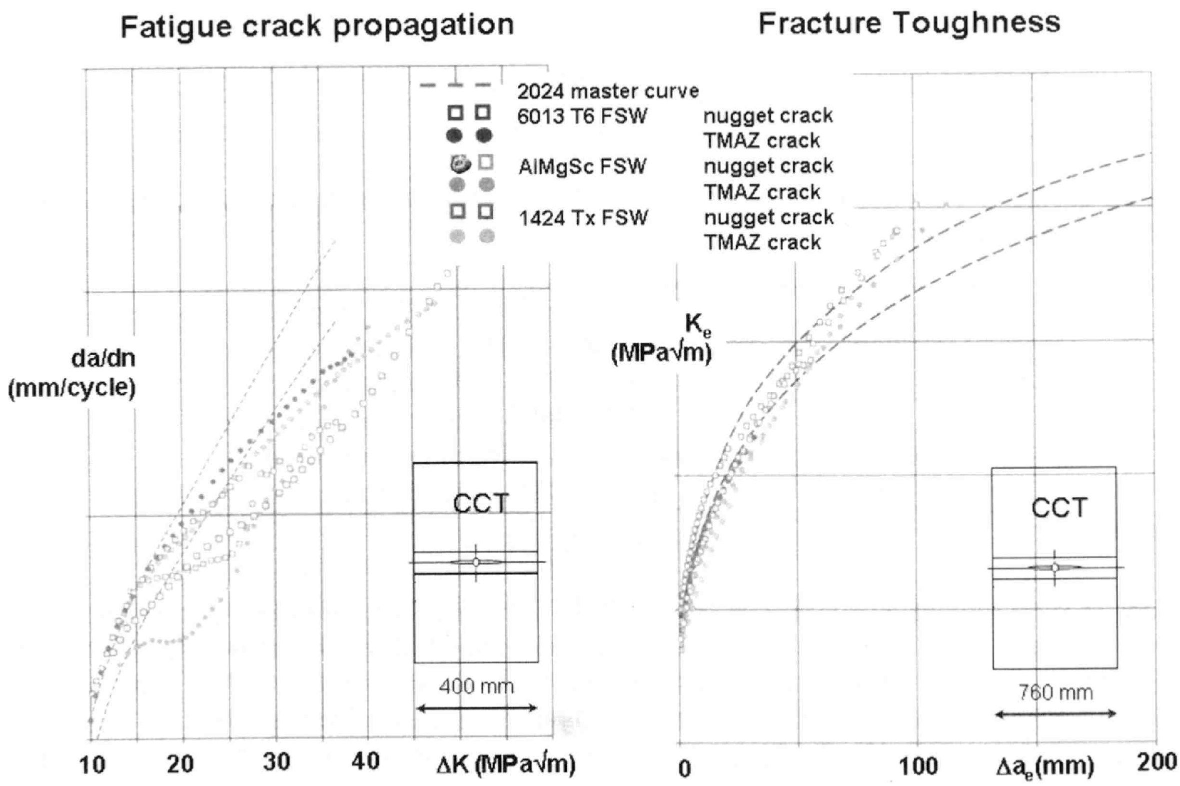

Figure 39: Crack growth and residual strength behavior of FSW joints

In frame of the research project TANGO (see above) curved panel tests have been carried out to investigate the crack propagation behavior of longitudinal FSW joints under internal pressure. The test panels are shown in Figure 40.

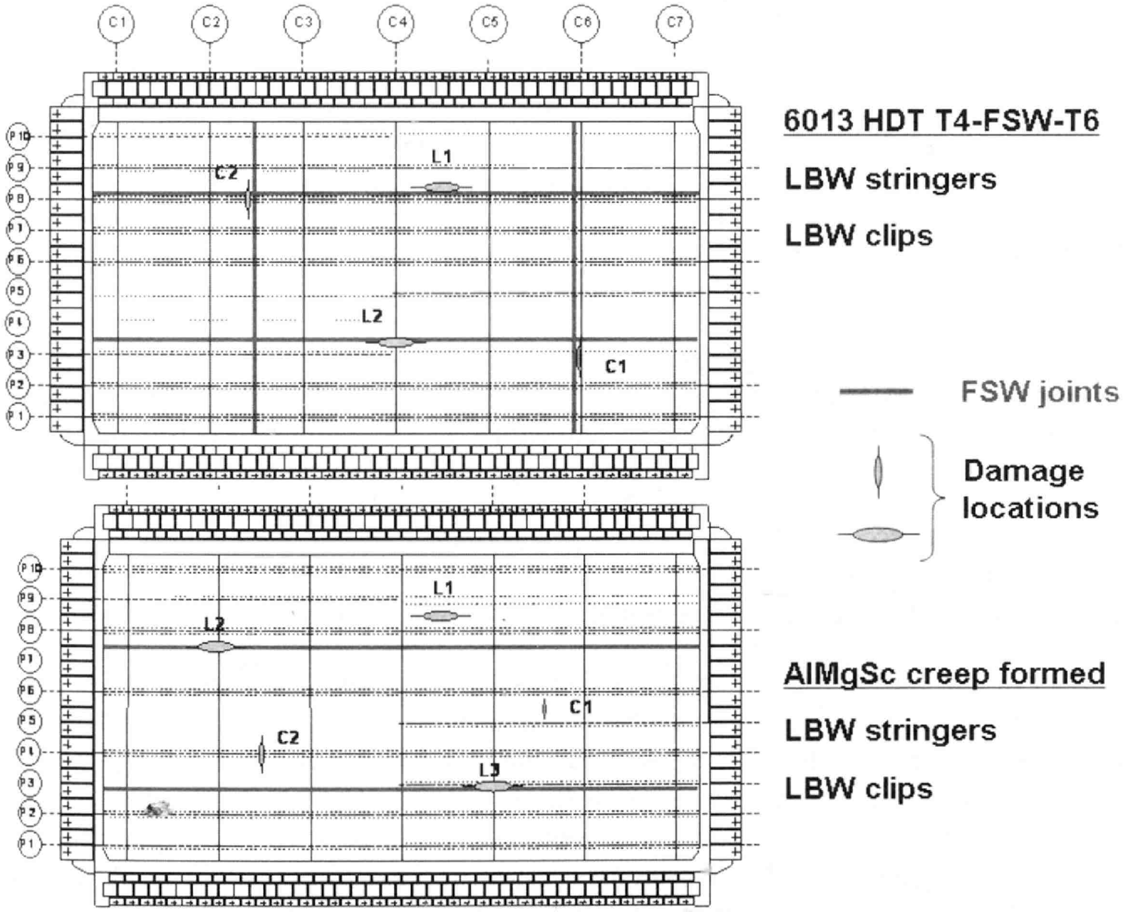

Figure 40: TANGO curved panel tests with FSW joints

These tests revealed the following results:

- Panel 6013 HDT T4-FSW-T6:
  - Longitudinal crack (L1) next to the stringer, see Figure 41:
    - stable slow crack propagation
  - Longitudinal crack (L2) halfway between the stringers, see Figure 41:
    - High bending on the weld seam (outer surface to inner surface 5:1)
    - Unstable crack propagation during fatigue cycling with Δp load
- Panel AlMgSc creep formed:
  - Crack growth in both, longitudinal and circumferential direction higher than expected (material properties were incorrect)
  - Good residual strength result

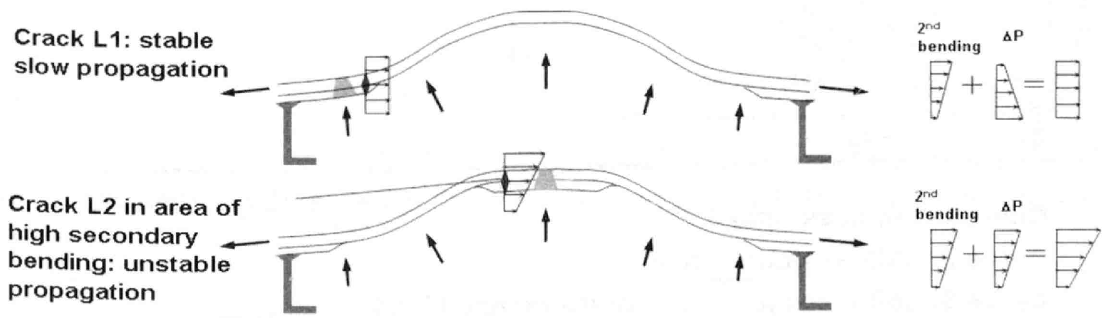

Figure 41: Crack growth behavior of FSW joints under internal pressure

4.4 Bonding / metal laminates

For weight reduction purposes several approaches are investigated to date. Even if bonding is no new technology, it is considered for structural improvements. Weight reduction may be achieved by using advanced bonded fuselage panels, especially in those areas, which are dimensioned by fatigue and damage tolerance. Further weight reduction will be achieved by increasing the stiffness ratio of the longitudinal stiffeners (stringer) and circumferential stiffeners (frames) and adding bonded straps and/or waffle plates to retard circumferential and longitudinal cracks.

Bonded features as straps and/or stringers, which are rectangular to the crack tip, provide significant better crack retardation than riveted features [24]. In addition the stiffness ratio of the skin / stiffener plays a major role for the crack retardation. The stiffness ratio is defined as

$$\mu = A_{stiffener} / (A_{stiffener} + A_{skin})$$

with:

$A_{stiffener}$ = area of stiffener

A_{skin} = area of skin per stiffener pitch, i.e. stiffener pitch multiplied by skin thickness

The effect of the stiffness ratio is given in Figure 42. It contains the general crack growth behavior of a circumferential skin crack above a broken bonded stringer. All adjacent stringers are bonded too. Curve 1 represents the crack growth behavior of the design with μ = 0.25. The allowable stress level is based on the value ΔN_A. The crack propagation period between the points A and A' has not been considered up to now, since this period has not been covered by former large panel tests. An increase of the stiffness ratio μ would lead to a slightly faster crack growth between detectable crack length and the point B, but to a significant longer period between B and B', see curve 2. However, the increase of the stiffness ratio is not the most weight effective solution to gain a longer period between B and B'. An increase of the area of the foot of the stringer or the application of an additional bonded doubler is much more efficient. However, the change of the stringer foot or the additional doubler leads to a very long period between B and B'. The allowable stress level is based on the value $\Delta N_{B'}$. Curve 3 represents the crack growth behavior in case of an increased stress level.

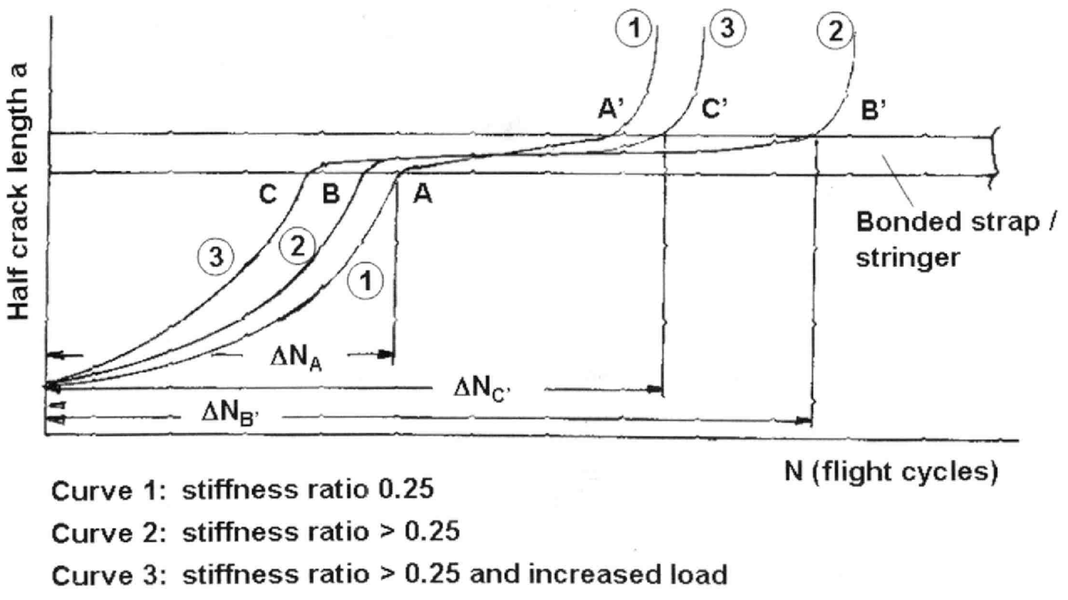

Figure 42: Effect of bonded straps and stiffness ratio on fatigue crack growth

A more advanced technology is the use of metal laminates [25]. They are produced by adhesive bonding of two or more thin sheets in order to obtain the required thickness. This laminate may be reinforced by bonded doublers and straps, which are located as necessary below or between the stiffeners, rectangular or with a specified other angle, see Figure 43.

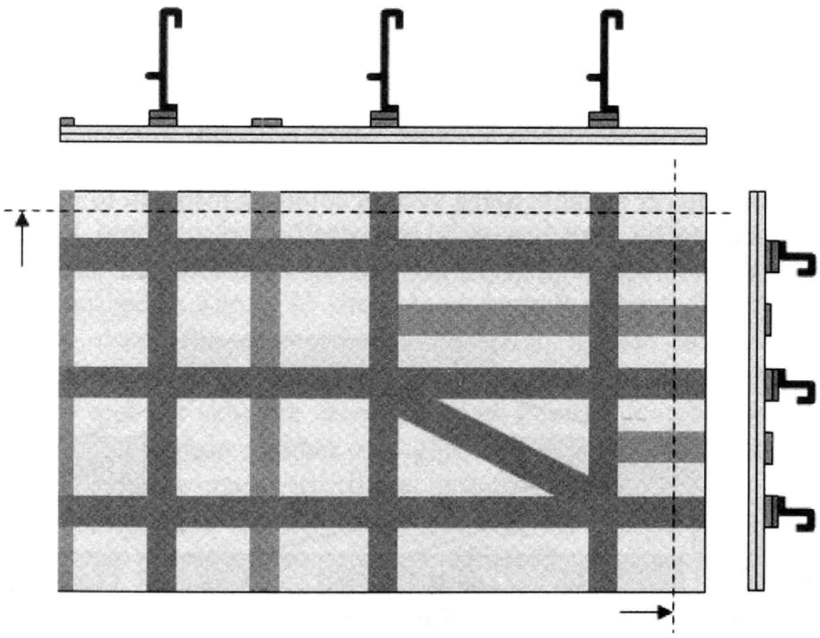

Figure 43: Principles of metal laminates

A superior behavior of metal laminates with respect to fatigue crack growth and fracture toughness results from the following facts:

- Thickness:
  Fatigue crack growth in thin sheets is slower than in thick sheets and plates.
- Peak load delay:
  Variable-amplitude loading produces larger plastic zones because in plane stress the plastic zone is larger in thin sheets and slower crack growth can be expected.
- Crack arrest:
  The adhesive layers and non-cracked sheets will retard crack growth in metal laminates.
- Additional crack stopper bands (strap):
  The crack stopper bands are applied in the aircraft fuselage to restrain the extent of fatigue cracking and to improve residual strength if cracks are present. The weight of crack stopper bands is relatively low. In order to be effective and reliable, and to be cost-effective as well, a high fatigue resistance of the crack stopper bands is essential.
- Surface crack:
  The penetration of part through (surface) cracks in the full thickness has a very slow crack growth rate in laminated materials compared to monolithic materials.

To limit manufacturing costs it is important to make an accurate choice of sheet thickness. Conceivable is the manufacturing of ML from the sheets with 0.6, 0.8 and 1.0 mm thickness.

However, it should be mentioned, that an excellent crack growth and residual strength behavior may also be reached, if a monolithic skin is used together with bonded doublers and straps.

4.5 Structural health monitoring

The application of structural health monitoring (SHM) may contribute significantly to reduce the aircraft weight and consequently the direct operating costs (DOCs). Furthermore it may be used to monitor hot spot areas for early damage detection and to perform crack monitoring. The expected weight reduction for monolithic aluminum structure results from a modification of today's damage tolerance philosophy, i.e. less stringent damage scenarios may be assumed in case of global SHM application. Figure 44 gives an overview about possible SHM applications for metallic structures and the major reasons for application [26]. In flying aircraft, there are known hot spot areas, which are sensitive to fatigue and/or stress corrosion or corrosion fatigue problems. A suitable SHM system could be installed to monitor these areas. The SHM application can be very beneficial, especially for structural locations which are difficult to inspect using conventional inspection methods and/or where access to the structure location is difficult.

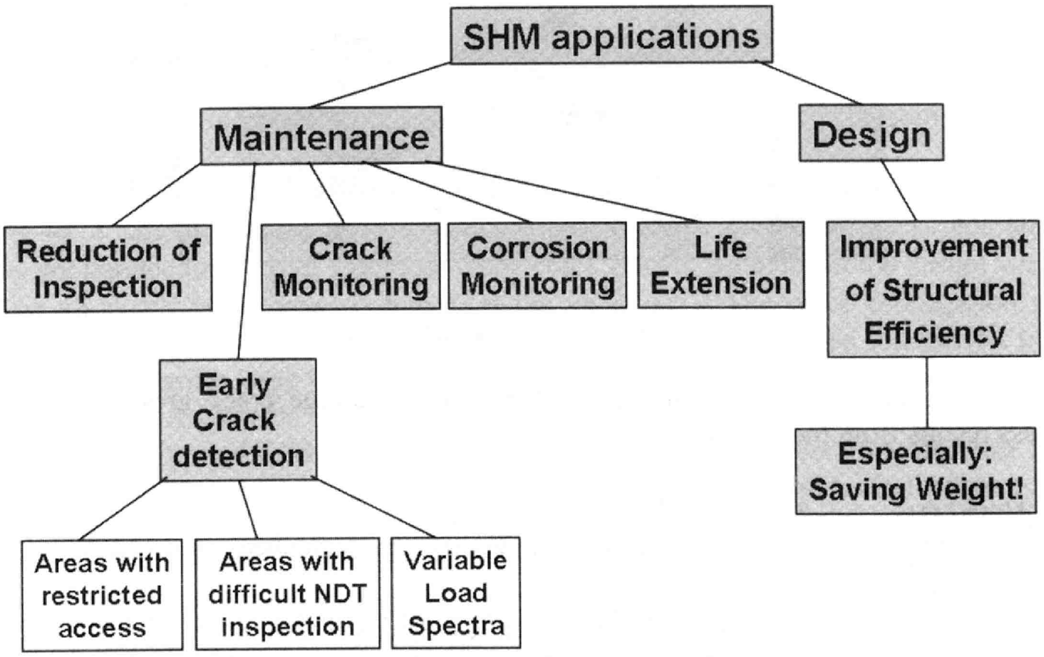

Figure 44: Overview of SHM application for metallic structures

The major benefit from SHM systems may be gained, if considered during the design of new aircraft. For improvement of the structural behavior it has to be checked, which design criterion may be improved by SHM. Table 8 contains the structural design criteria and the possible improvements by SHM.

Criteria	Change due to SHM application
Static strength	No improvement possible
Fatigue strength (durability)	No improvement possible
Airworthiness	Improvements possible, but current structure meets airworthiness requirements
Crack growth periods	Improvements in case of longer cracks due to modified crack scenarios
Structural damage capability	Improvements in case of fatigue cracks due to modified crack scenarios, no improvements possible for impact damage due to accidental damage scenario

Table 8: Challenging of design criteria by SHM

The benefits due to SHM mentioned above exist in metallic areas dimensioned by damage tolerance, i.e. mainly by crack growth. These areas are dependent on the aircraft type, design criteria, mission profile, inspection program and material. There are four major different possibilities of SHM application at fuselage structure:

- monitoring of stringers – to detect stringer cracks or failures
- monitoring of frames – to detect frame cracks or failures
- monitoring of skin – to detect circumferential skin cracks
- monitoring of skin – to detect longitudinal skin cracks

As one of the first possible applications the monitoring of internal stiffeners in wing or fuselage panels is investigated. The effects of a health monitoring system on the inspection requirements is described in Figure 45 showing an aircraft wing or fuselage skin stiffened by stringers. In many cases the conventional inspection system does not require internal inspections of the stringers. For these cases it is assumed that the stringer contains the so-called primary flaw and the skin the secondary flaw (shorter length than the primary flaw). The stringer fails after a certain number of flights; afterwards the loads are redistributed into the skin, which increases the crack growth rate in the skin. The inspection interval is based on the crack growth period between the detectable and the critical crack length in the skin divided by an appropriate scatter factor. In case of health monitoring of the stringer a failure of the stringer has not to be assumed (i.e. the stringer is intact), which reduces the crack growth rate in the skin significantly. The crack growth period between 2a = 75 mm, which is detectable by general visual inspection of the fuselage, and the critical crack length is increased by a factor of roughly 2.5. This would either allow to increase the intervals for general visual inspection by this factor or to increase the allowable stress level by more than 15 percent. This significant improvement is not applicable for areas dimensioned by other design criteria, e.g. static strength.

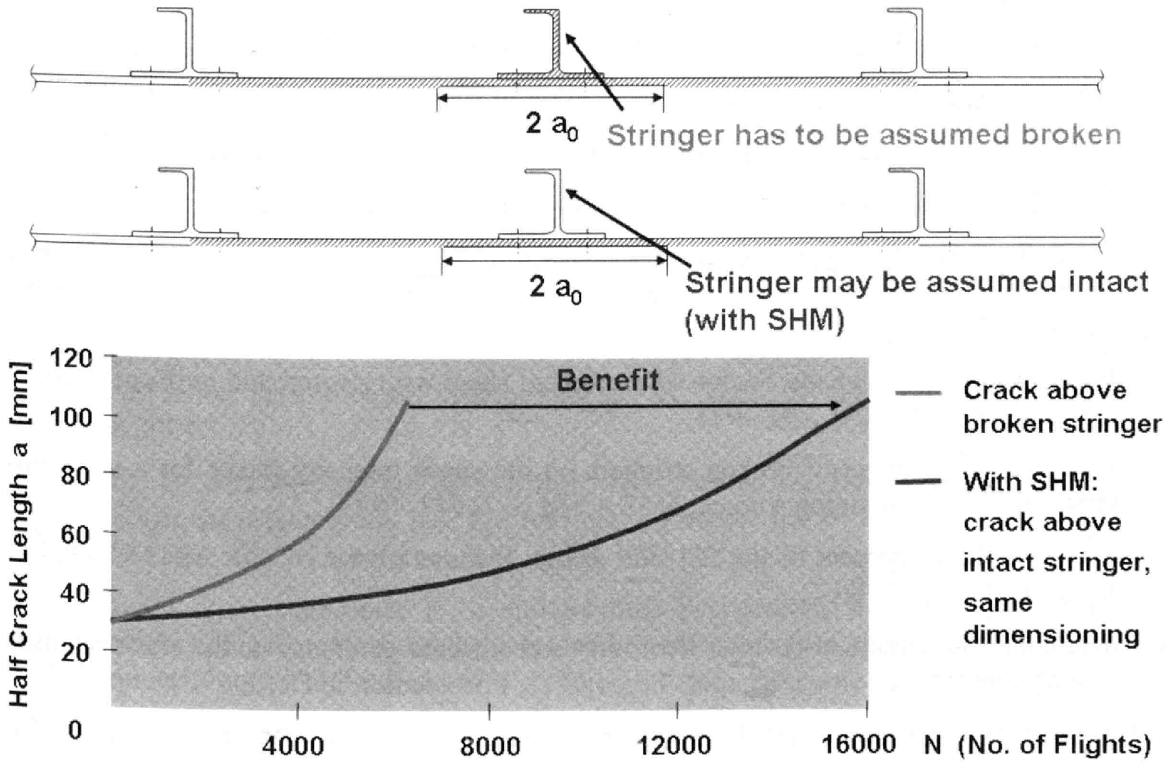

Figure 45: Example for SHM application – stringer monitoring

5 CONCLUSION

The current fatigue and damage tolerance technologies for built-up structure are well defined leading to low weight, low manufacturing and operational costs and the envisaged airworthiness. These technologies have been successfully extended to hybrid (GLARE®) and welded structure (e.g. LBW), which are applied beneficially in specific fuselage areas according to their advanced properties. Reliable analysis methods have been developed and successfully applied to multiple site damage and multiple element damage scenarios, which are a special concern in fatigue and damage tolerance for aging aircraft and new design.
Further improvements and extension of the fatigue and damage tolerance technologies are required for the next generation of metallic fuselage structure, which have to compete with composite designs. The analysis methods must be able to predict exactly the structural behavior of advanced hybrid, integral and welded structure made of the next generation of materials. For the future structure analysis a combination of deterministic and probabilistic analysis is essential, since initial damage scenarios are of a probabilistic nature as well as loads and materials properties.

Fatigue and damage tolerance analysis methodologies are significantly supported by testing, whereby large components, such as curved panels and barrels, as well as full scale fatigue tests play a major role. In the future some tests may be substituted by virtual testing using advanced computational methods and the experience in the field of fatigue and damage tolerance made during the last fifty years.

Additional improvements to the fatigue and damage tolerance behavior are expected due to the application of structural health monitoring. Fatigue and damage tolerance considerations will allow to quantify and to verify the benefits regarding structural weight, maintenance and reliability improvements.

6 REFERENCES

/1/ N.N., Damage tolerance and fatigue evaluation of structure, FAR 25.571 Amendment 96

/2/ N.N., Damage tolerance and fatigue evaluation of structure, AC 25.571-1C

/3/ N.N., Damage tolerance and fatigue evaluation of structure, draft rule 25.571

/4/ N.N., Damage tolerance and fatigue evaluation of structure, Draft AC 25.571-1x

/5/ Swift, T., Fail-safe design requirements and features, regulatory requirements, presented at the International Air & Space Symposium and Exhibition "The Next 100 Years", Dayton, USA, July 2003

/6/ Poe, C.C., Stress-intensity Factor for a cracked sheet with riveted and uniformly spaced stringers, NASA TR R-358, 1971

/7/ Poe, C.C., The effect of broken stringers on the stress intensity factor for a uniformly stiffened sheet containing a crack, NASA TM X-71947, 1973

/8/ Swift, T., Development of the fail-safe design features of the DC-10, ASTM STP 486, pp. 164-214, 1971

/9/ Swift, T., The effects of fastener flexibility and stiffener geometry on the stress intensity in stiffened cracked sheet, Douglas Paper 6211, Presentation in Delft, 1974

/10/ Ahmed, S., van Nieuwendijk, H., Cracked Stiffened Panels, Airbus, Hamburg, Germany, November 2000 (unpublished)

/11/ Swift, T., Fracture analysis of Stiffened Structure, Damage Tolerance of Metallic Structure: Analysis methods and Application, ASTM STP 842, pp. 69-107, 1984

/12/ N.N., Recommendations for Regulatory Action to Prevent Widespread Fatigue Damage in the Commercial Airplane Fleet, A report of the Airworthiness Assurance Working Group, final report, revision A, June 1999

/13/ Horst, P. and Schmidt, H.-J., On the Significance of Probabilistic Parameters for the Assessment of MSD in the Case of Aging Aircraft, 19th Congress of the International Council of the Aeronautical Sciences (ICAS), Anaheim, CA., USA, September 1994

/14/ Schmidt, H.-J., Airbus A300 Fuselage, Program for Life Extension and Widespread Fatigue Damage Evaluation, The Third Joint FAA/DoD/NASA Conference on Aging Aircraft, Albuquerque, New Mexico, USA, September 1999

/15/ Trey, H., EADS Airbus GmbH Tool for Widespread Fatigue Damage Evaluation – MSDSim, Presentation at EADS Airbus GmbH, Hamburg, Germany, May, 2001 (unpublished)

/16/ Schmidt, H.-J. and Schmidt-Brandecker, B., Current Status of Research and Development Activities for the Fuselage of a Large Airbus Aircraft, presented at the 20th ICAF Symposium, Bellevue, WA., USA, July 1999

/17/ Beumler, T., GLARE – Werkstoffkonzept und Struktureigenschaften, presented at ILA Werkstofftag, Berlin, Germany 2002

/18/ Homan, J., Damage Tolerance Analysis in Glare, Presentation at Airbus, Faculty of Aerospace Engineering, Delft University of Technology, The Netherlands, 2002 (unpublished)

/19/ Vries, T.J. de, Blunt and sharp notch behaviour of Glare laminates, Ph.D. Thesis, Delft University of Technology, The Netherlands, 2001

/20/ Müller, R.P.G., An experimental and analytical investigation on the fatigue behaviour of fuselage riveted joints, Ph.D. Thesis, Delft University of Technology, The Netherlands, 1995

/21/ Schmidt, H.-J. and Schmidt-Brandecker, B., Damage Tolerant Design and Analysis of Current and Future Aircraft Structure, Presented at „The Next 100 Years" AIAA/ICAS International Air and Space Symposium, Dayton, O.H., USA, July 2003

/22/ Pacchione, M., The challenges of the integral metallic fuselage, Presented at DVM Symposium, Ottobrunn, Germany, January 2005

/23/ Schmidt, H.-J., Voto, C. and Hansson, J., TANGO Metallic Fuselage Barrel - Validation of Advanced Technologies, Presented at the 21st ICAF Symposium, Toulouse, France, June 2001

/24/ Swift, T., The Application of Fracture Mechanics in the Development of the DC-10 Fuselage, AGARDograph No. 176 on Fracture Mechanics of Aircraft Structures, edited by H. Liebowitz, Washington, D.C., USA, 1974

/25/ Vichniakov, A., Schmidt, H.-J. and Schmidt-Brandecker, B., Numerical analysis of crack growth phenomena in the airplane structures, Presented at the 7th International Seminar "Numerical Analysis of Weldability", Graz – Seggau, Austria, September 2003

/26/ Schmidt, H.-J., Telgkamp, J. and Schmidt-Brandecker, B., Application of Structural Health Monitoring to Improve Efficiency of Aircraft Structure, Presented at the European Workshop on Structural Health Monitoring, Munich, Germany, July 2004